INTERNATIONAL STANDARD

ISO 10300-1

Second edition
2014-04-01

Calculation of load capacity of bevel gears —

Part 1:
Introduction and general influence factors

Calcul de la capacité de charge des engrenages coniques —

Partie 1: Introduction et facteurs généraux d'influence

Reference number
ISO 10300-1:2014(E)

Contents

Page

Foreword

ISO (the International Organization for Standardization) is a worldwide federation of national standards bodies (ISO member bodies). The work of preparing International Standards is normally carried out through ISO technical committees. Each member body interested in a subject for which a technical committee has been established has the right to be represented on that committee. International organizations, governmental and non-governmental, in liaison with ISO, also take part in the work. ISO collaborates closely with the International Electrotechnical Commission (IEC) on all matters of electrotechnical standardization.

The procedures used to develop this document and those intended for its further maintenance are described in the ISO/IEC Directives, Part 1. In particular the different approval criteria needed for the different types of ISO documents should be noted. This document was drafted in accordance with the editorial rules of the ISO/IEC Directives, Part 2. www.iso.org/directives

Attention is drawn to the possibility that some of the elements of this document may be the subject of patent rights. ISO shall not be held responsible for identifying any or all such patent rights. Details of any patent rights identified during the development of the document will be in the Introduction and/or on the ISO list of patent declarations received. www.iso.org/patents

Any trade name used in this document is information given for the convenience of users and does not constitute an endorsement.

For an explanation on the meaning of ISO specific terms and expressions related to conformity assessment, as well as information about ISO's adherence to the WTO principles in the Technical Barriers to Trade (TBT) see the following URL: Foreword - Supplementary information

The committee responsible for this document is ISO/TC 60, *Gears*, Subcommittee SC 2, *Gear capacity calculation*.

This second edition cancels and replaces the first edition (ISO 10300-1:2001), which has been technically revised.

ISO 10300 consists of the following parts, under the general title *Calculation of load capacity of bevel gears*:

— *Part 1: Introduction and general influence factors*

— *Part 2: Calculation of surface durability (pitting)*

— *Part 3: Calculation of tooth root strength*

Introduction

When ISO 10300:2001 (all parts, withdrawn) became due for (its first) revision, the opportunity was taken to include hypoid gears, since previously the series only allowed for calculating the load capacity of bevel gears without offset axes. The former structure is retained, i.e. three parts of the ISO 10300 series, together with ISO 6336-5, and it is intended to establish general principles and procedures for rating of bevel gears. Moreover, ISO 10300 (all parts) is designed to facilitate the application of future knowledge and developments, as well as the exchange of information gained from experience.

Several calculation methods, i.e. A, B and C, are specified, which stand for decreasing accuracy and reliability from A to C because of simplifications implemented in formulae and factors. The approximate methods in ISO 10300 (all parts) are used for preliminary estimates of gear capacity where the final details of the gear design are not yet known. More detailed methods are intended for the recalculation of the load capacity limits when all important gear data are given.

ISO 10300 (all parts) does not provide an upgraded calculation procedure as a method A, although it would be available, such as finite element or boundary element methods combined with sophisticated tooth contact analyses. The majority of Working Group 13 decided that neither is it sufficient for an International Standard to simply refer to such a complex computer program, nor does it make sense to explain it step by step in an International Standard.

On the other hand, by means of such a computer program, a new calculation procedure for bevel and hypoid gears on the level of method B was developed and checked. It is part of the ISO 10300 series as submethod B1. Besides, if the hypoid offset, a, is zero, method B1 becomes identical to the set of proven formulae of the former version of ISO 10300 (all parts):2001.

In view of the decision for ISO 10300 (all parts) to cover hypoid gears also, an annex, called: “Calculation of virtual cylindrical gears — Method B2”, is included in this part of ISO 10300. Additionally, ISO 10300-2 is supplemented by a separate clause: “Gear flank rating formulae — Method B2”; regarding ISO 10300-3, it was agreed that the former method B2, which uses the Lewis parabola to determine the critical section in the root and not the 30° tangent at the tooth fillet as method B1 does, now be extended by the AGMA methods for rating the strength of bevel gears and hypoid gears. It was necessary to present a new, clearer structure of the three parts, which is illustrated in Figure 1 (of this part of ISO 10300). Note, ISO 10300 (all parts) gives no preferences in terms of when to use method B1 and when method B2.

The procedures covered by ISO 10300 (all parts) are based on both testing and theoretical studies, but it is possible that the results obtained from its rating calculations might not be in good agreement with certain, previously accepted, gear calculation methods.

ISO 10300 (all parts) provides calculation procedures by which different gear designs can be compared. It is neither meant to ensure the performance of assembled gear drive systems nor intended for use by the average engineer. Rather, it is aimed at the experienced gear designer capable of selecting reasonable values for the factors in these formulae, based on knowledge of similar designs and on awareness of the effects of the items discussed.

NOTE Contrary to cylindrical gears, where the contact is usually linear, bevel gears are generally manufactured with profile and lengthwise crowning: i.e. the tooth flanks are curved on all sides and the contact develops an elliptical pressure surface. This is taken into consideration when determining the load factors by the fact that the rectangular zone of action (in the case of spur and helical gears) is replaced by an inscribed parallelogram for method B1 and an inscribed ellipse for method B2 (see Annex A for method B1 and Annex B for method B2). The conditions for bevel gears, different from cylindrical gears in their contact, are thus taken into consideration by the longitudinal and transverse load distribution factors.

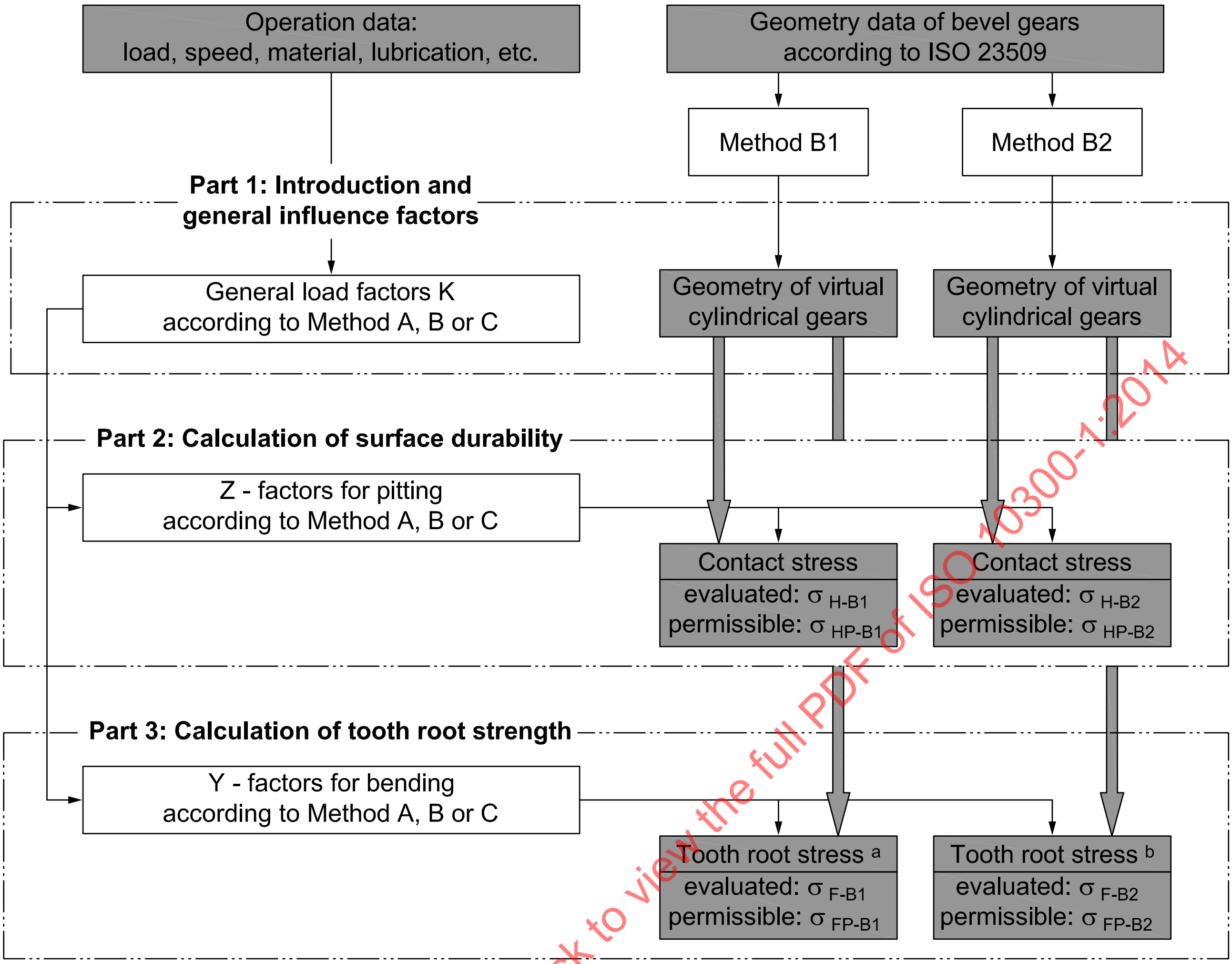

Key

a One set of formulae for both, bevel and hypoid gears.

b Separate sets of formulae for bevel and for hypoid gears.

Figure 1 — Structure of calculation methods in ISO 10300 (all parts)

Calculation of load capacity of bevel gears —

Part 1:
Introduction and general influence factors

1 Scope

This part of ISO 10300 specifies the methods of calculation of the load capacity of bevel gears, the formulae and symbols used for calculation, and the general factors influencing load conditions.

The formulae in ISO 10300 (all parts) are intended to establish uniformly acceptable methods for calculating the pitting resistance and bending strength of straight, helical (skew), spiral bevel, Zerol and hypoid gears. They are applicable equally to tapered depth and uniform depth teeth. Hereinafter, the term “bevel gear” refers to all of these gear types; if not the case, the specific forms are identified.

The formulae take into account the known major factors influencing pitting on the tooth flank and fractures in the tooth root. The rating formulae are not applicable to other types of gear tooth deterioration such as plastic yielding, micropitting, case crushing, welding, and wear. The bending strength formulae are applicable to fractures at the tooth fillet, but not to those on the active flank surfaces, to failures of the gear rim or of the gear blank through the web and hub. Pitting resistance and bending strength rating systems for a particular type of bevel gears can be established by selecting proper values for the factors used in the general formulae. If necessary, the formulae allow for the inclusion of new factors at a later date. Note, ISO 10300 (all parts) is not applicable to bevel gears which have an inadequate contact pattern under load (see Annex D).

The rating system of ISO 10300 (all parts) is based on virtual cylindrical gears and restricted to bevel gears whose virtual cylindrical gears have transverse contact ratios of $\varepsilon_{v\alpha} < 2$. Additionally, the given relations are valid for bevel gears of which the sum of profile shift coefficients of pinion and wheel is zero (see ISO 23509).

WARNING — The user is cautioned that when the formulae are used for large average mean spiral angles $(\beta_{m1}+\beta_{m2})/2 > 45°$, for effective pressure angles $\alpha_e > 30°$ and/or for large face widths $b > 13\ m_{mn}$, the calculated results of ISO 10300 (all parts) should be confirmed by experience.

2 Normative references

The following documents, in whole or in part, are normatively referenced in this document and are indispensable to its application. For dated references, only the edition cited applies. For undated references, the latest edition of the referenced document (including any amendments) applies.

ISO 1122-1, *Vocabulary of gear terms — Part 1: Definitions related to geometry*

ISO 6336-5, *Calculation of load capacity of spur and helical gears — Part 5: Strength and quality of materials*

ISO 10300-2:2014, *Calculation of load capacity of bevel gears — Part 2: Calculation of surface durability (pitting)*

ISO 10300-3:2014, *Calculation of load capacity of bevel gears — Part 3: Calculation of tooth root strength*

ISO 17485, *Bevel gears — ISO system of accuracy*

ISO 23509:2006, *Bevel and hypoid gear geometry*

3 Terms and definitions

For the purposes of this part of ISO 10300, terms and definitions given in ISO 1122-1 and ISO 23509 apply.

4 Symbols and units

For the purposes of this document, the symbols given in ISO 701, ISO 17485 and ISO 23509 apply.

Table 1 contains symbols and their units which are used at more than one places of ISO 10300 (all parts). Other symbols, especially those of auxiliary variables, which are used in equations following closely after their definitions, are not listed in Table 1. Table 2 contains general subscripts used in ISO 10300 (all parts).

Table 1 — Symbols and units used in ISO 10300 (all parts)

Symbol	Description or term	Unit
a	hypoid offset	mm
a_{rel}	relative hypoid offset	—
a_v	centre distance of virtual cylindrical gear pair	mm
a_{vn}	centre distance of virtual cylindrical gear pair in normal section	mm
b	face width	mm
b_b	relative base face width	—
b_{ce}	calculated effective face width	mm
b_{eff}	effective face width (e.g. measured length of contact pattern)	mm
b_v	face width of virtual cylindrical gears	mm
$b_{v,eff}$	effective face width of virtual cylindrical gears	mm
c_v	empirical parameter to determine the dynamic factor	—
c_γ	mean value of mesh stiffness per unit face width	N/(mm · µm)
$c_{\gamma 0}$	mesh stiffness for average conditions	N/(mm · µm)
c'	single stiffness	N/(mm · µm)
c_0'	single stiffness for average conditions	N/(mm · µm)
d_e	outer pitch diameter	mm
d_m	mean pitch diameter	mm
d_T	tolerance diameter according to ISO 17485	mm
d_v	reference diameter of virtual cylindrical gear	mm
d_{va}	tip diameter of virtual cylindrical gear	mm
d_{van}	tip diameter of virtual cylindrical gear in normal section	mm
d_{vb}	base diameter of virtual cylindrical gear	mm
d_{vbn}	base diameter of virtual cylindrical gear in normal section	mm
d_{vf}	root diameter of virtual cylindrical gear	mm
d_{vn}	reference diameter of virtual cylindrical gear in normal section	mm
e	exponent for the distribution of the load peaks along the lines of contact	—
f	distance from the centre of the zone of action to a contact line	mm
f_{max}	maximum distance to middle contact line	mm
f_{maxB}	maximum distance to middle contact line at right side of contact pattern	mm
f_{max0}	maximum distance to middle contact line at left side of contact pattern	mm

Table 1 *(continued)*

Symbol	Description or term	Unit
f_{pt}	single pitch deviation	µm
$f_{p,eff}$	effective pitch deviation	µm
g_c	length of contact line (method B2)	mm
$g_{v\alpha}$	length of path of contact of virtual cylindrical gear in transverse section	mm
$g_{v\alpha n}$	relative length of action in normal section	—
g_J	relative length of action to point of load application (method B2)	—
g_η	relative length of action within the contact ellipse	—
h_{am}	mean addendum	mm
h_{a0}	tool addendum	mm
h_{fm}	mean dedendum	mm
h_{fP}	dedendum of the basic rack profile	mm
h_m	mean whole depth used for bevel spiral angle factor	mm
h_{vfm}	relative mean virtual dedendum	—
h_{Fa}	bending moment arm for tooth root stress (load application at tooth tip)	mm
h_N	load height from critical section (method B2)	mm
k'	contact shift factor	—
l_b	length of contact line (method B1)	mm
l_{b0}	theoretical length of contact line	mm
l_{bm}	theoretical length of middle contact line	mm
m_{et}	outer transverse module	mm
m_{mn}	mean normal module	mm
m_{mt}	mean transverse module	mm
m_{red}	mass per unit face width reduced to the line of action of dynamically equivalent cylindrical gears	kg/mm
m^*	relative individual gear mass per unit face width referred to line of action	kg/mm
n	rotational speed	min^{-1}
n_{E1}	resonance speed of pinion	min^{-1}
p	peak load	N/mm
p_{et}	transverse base pitch (method B2)	mm
p_{max}	maximum peak load	N/mm
p^*	relative peak load for calculating the load sharing factor (method B1)	—
p_{mn}	relative mean normal pitch	—
p_{nb}	relative mean normal base pitch	—
p_{vet}	transverse base pitch of virtual cylindrical gear (method B1)	mm
q	exponent in the formula for lengthwise curvature factor	—
q_s	notch parameter	—
r_{c0}	cutter radius	mm
r_{mf}	tooth fillet radius at the root in mean section	mm
r_{mpt}	mean pitch radius	mm
$r_{my\,0}$	mean transverse radius to point of load application (method B2)	mm
r_{va}	relative mean virtual tip radius	—

Table 1 *(continued)*

Symbol	Description or term	Unit
r_{vn}	relative mean virtual pitch radius	—
s_{mn}	mean normal circular thickness	mm
s_{pr}	amount of protuberance at the tool	mm
s_{Fn}	tooth root chord in calculation section	mm
s_{N}	one-half tooth thickness at critical section (method B2)	mm
u	gear ratio of bevel gear	—
u_{v}	gear ratio of virtual cylindrical gear	—
v_{et}	tangential speed at outer end (heel) of the reference cone	m/s
$v_{\mathrm{et,max}}$	maximum pitch line velocity at operating pitch diameter	m/s
v_{g}	sliding velocity in the mean point P	m/s
$v_{\mathrm{g,par}}$	sliding velocity parallel to the contact line	m/s
$v_{\mathrm{g,vert}}$	sliding velocity vertical to the contact line	m/s
v_{mt}	tangential speed at mid-face width of the reference cone	m/s
v_{Σ}	sum of velocities in the mean point P	m/s
$v_{\Sigma\mathrm{h}}$	sum of velocities in profile direction	m/s
$v_{\Sigma\mathrm{l}}$	sum of velocities in lengthwise direction	m/s
$v_{\Sigma,\mathrm{vert}}$	sum of velocities vertical to the contact line	m/s
w	angle of contact line relative to the root cone	°
x_{hm}	profile shift coefficient	—
x_{sm}	thickness modification coefficient	—
x_{N}	tooth strength factor (method B2)	mm
x_{oo}	distance from mean section to point of load application	mm
y_{p}	running-in allowance for pitch deviation related to the polished test piece	µm
y_{J}	location of point of load application for maximum bending stress on path of action (method B2)	mm
y_3	location of point of load application on path of action for maximum root stress	mm
y_{α}	running-in allowance for pitch error	µm
z	number of teeth	—
z_{v}	number of teeth of virtual cylindrical gear	—
z_{vn}	number of teeth of virtual cylindrical gear in normal section	—
z_0	number of blade groups of the cutter	—
A	auxiliary factor for calculating the dynamic factor $K_{\mathrm{v\text{-}C}}$	—
A^*	related area for calculating the load sharing factor Z_{LS}	mm
A_{sne}	outer tooth thickness allowance	mm
B	accuracy grade according to ISO 17485	—
C_{F}	correction factor of tooth stiffness for non average conditions	—
C_{lb}	correction factor for the length of contact lines	—
C_{ZL}, C_{ZR}, C_{ZV}	constants for determining lubricant film factors	—
E	modulus of elasticity, Young's modulus	$\mathrm{N/mm^2}$
E, G, H	auxiliary variables for tooth form factor (method B1)	—

Table 1 *(continued)*

Symbol	Description or term	Unit
F	auxiliary variable for mid-zone factor	—
F_{mt}	nominal tangential force at mid-face width of the reference cone	N
F_{mtH}	determinant tangential force at mid-face width of the reference cone	N
F_n	nominal normal force	N
F_{vmt}	nominal tangential force of virtual cylindrical gears	N
HB	Brinell hardness	—
K	constant; factor for calculating the dynamic factor K_{v-B}	—
K_v	dynamic factor	—
K_v*	preliminary dynamic factor for non-hypoid gears	—
K_A	application factor	—
K_{F0}	lengthwise curvature factor for bending stress	—
$K_{F\alpha}$	transverse load factor for bending stress	—
$K_{F\beta}$	face load factor for bending stress	—
$K_{H\alpha}$	transverse load factor for contact stress	—
$K_{H\alpha}$*	preliminary transverse load factor for contact stress for non-hypoid gears	—
$K_{H\beta}$	face load factor for contact stress	—
$K_{H\beta\text{-be}}$	mounting factor	—
N	reference speed related to resonance speed n_{E1}	—
N_L	number of load cycles	—
P	nominal power	kW
Ra	= CLA = AA arithmetic average roughness	µm
R_e	outer cone distance	mm
R_m	mean cone distance	mm
R_{mpt}	relative mean back cone distance	—
Rz	mean roughness	µm
Rz_{10}	mean roughness for gear pairs with relative curvature radius ρ_{rel} = 10 mm	µm
S_F	safety factor for bending stress (against breakage)	—
$S_{F,min}$	minimum safety factor for bending stress	—
S_H	safety factor for contact stress (against pitting)	—
$S_{H,min}$	minimum safety factor for contact stress	—
$T_{1,2}$	nominal torque of pinion and wheel	Nm
W_{m2}	wheel mean slot width	mm
$Y_{1,2}$	tooth form factor of pinion and wheel (method B2)	—
Y_f	stress concentration and stress correction factor (method B2)	—
Y_i	inertia factor (bending)	—
Y_A	root stress adjustment factor (method B2)	—
Y_{BS}	bevel spiral angle factor	—
Y_{Fa}	tooth form factor for load application at the tooth tip (method B1)	—
Y_{FS}	combined tooth form factor for generated gears	—
Y_J	bending strength geometry factor (method B2)	—
Y_{LS}	load sharing factor (bending)	—

Table 1 *(continued)*

Symbol	Description or term	Unit
Y_{NT}	life factor (bending)	—
$Y_{R,Rel\,T}$	relative surface condition factor	—
Y_{Sa}	stress correction factor for load application at the tooth tip	—
Y_{ST}	stress correction factor for dimensions of the standard test gear	—
Y_X	size factor for tooth root stress	—
$Y_{\delta,rel\,T}$	relative notch sensitivity factor	—
Y_ε	contact ratio factor for bending (method B1)	—
Z_i	inertia factor (pitting)	—
Z_v	speed factor	—
Z_A	contact stress adjustment factor (method B2)	—
Z_E	elasticity factor	$(N/mm^2)^{1/2}$
Z_{FW}	face width factor	—
Z_{Hyp}	hypoid factor	—
Z_I	pitting resistance geometry factor (method B2)	—
Z_K	bevel gear factor (method B1)	—
Z_L	lubricant factor	—
Z_{LS}	load sharing factor (method B1)	—
$Z_{M\text{-}B}$	mid-zone factor	—
Z_{NT}	life factor (pitting)	—
Z_R	roughness factor for contact stress	—
Z_S	bevel slip factor	—
Z_W	work hardening factor	—
Z_X	size factor	—
α_a	adjusted pressure angle (method B2)	°
α_{an}	normal pressure angle at tooth tip	°
α_{et}	effective pressure angle in transverse section	°
$\alpha_{eD,C}$	effective pressure angle for drive side/coast side	°
α_f	limit pressure angle in wheel root coordinates (method B2)	°
α_{lim}	limit pressure angle	°
$\alpha_{nD,C}$	generated pressure angle for drive side/coast side	°
α_{vet}	transverse pressure angle of virtual cylindrical gears	°
α_{Fan}	load application angle at tooth tip of virtual cylindrical gear (method B1)	°
α_L	normal pressure angle at point of load application (method B2)	°
β_{bm}	mean base spiral angle	°
β_m	mean spiral angle	°
β_v	helix angle of virtual gear (method B1), virtual spiral angle (method B2)	°
β_{vb}	helix angle at base circle of virtual cylindrical gear	°
β_B	inclination angle of contact line	°
γ	auxiliary angle for length of contact line calculation (method B1)	°
γ'	projected auxiliary angle for length of contact line	°
γ_a	auxiliary angle for tooth form and tooth correction factor	°

Table 1 *(continued)*

Symbol	Description or term	Unit
δ	pitch angle of bevel gear	°
δ_a	face angle	°
δ_f	root angle	°
$\varepsilon_{v\alpha}$	transverse contact ratio of virtual cylindrical gears	—
$\varepsilon_{v\alpha n}$	transverse contact ratio of virtual cylindrical gears in normal section	—
$\varepsilon_{v\beta}$	face contact ratio of virtual cylindrical gears	—
$\varepsilon_{v\gamma}$	virtual contact ratio (method B1), modified contact ratio (method B2)	—
ε_N	load sharing ratio for bending (method B2)	—
ε_{NI}	load sharing ratio for pitting (method B2)	—
ζ_m	pinion offset angle in axial plane	°
ζ_{mp}	pinion offset angle in pitch plane	°
ζ_R	pinion offset angle in root plane	°
ϑ	auxiliary quantity for tooth form and tooth correction factors	radiant
ϑ_{mp}	auxiliary angle for virtual face width (method B1)	°
θ_{v2}	angular pitch of virtual cylindrical wheel	radiant
ξ	assumed angle in locating weakest section	radiant
ξ_h	one half of angle subtended by normal circular tooth thickness at point of load application	radiant
ρ	density of gear material	kg/mm^3
ρ_{a0}	cutter edge radius	mm
ρ_F	fillet radius at point of contact of 30° tangent	mm
ρ_{Fn}	fillet radius at point of contact of 30° tangent in normal section	mm
ρ_{fP}	root fillet radius of basic rack for cylindrical gears	mm
ρ_{rel}	radius of relative curvature vertical to contact line at virtual cylindrical gears	mm
ρ_t	relative radius of profile curvature between pinion and wheel (method B2)	—
ρ_{va0}	relative edge radius of tool	—
ρ'	slip layer thickness	mm
σ_F	tooth root stress	N/mm^2
$\sigma_{F,lim}$	nominal stress number (bending)	N/mm^2
σ_{FE}	allowable stress number (bending)	N/mm^2
σ_{FP}	permissible tooth root stress	N/mm^2
σ_H	contact stress	N/mm^2
$\sigma_{H,lim}$	allowable stress number for contact stress	N/mm^2
σ_{HP}	permissible contact stress	N/mm^2
τ	angle between tangent of root fillet at weakest point and centreline of tooth	°
ν	Poisson's ratio	—
ν_0	lead angle of face hobbing cutter	°
ν_{40}, ν_{50}	nominal kinematic viscosity of the oil at 40 °C and 50 °C respectively	mm^2/s
φ	auxiliary angle to determine the position of the pitch point	°
ω	angular velocity	rad/s

Table 1 *(continued)*

Symbol	Description or term	Unit
ω_Σ	angle between the sum of velocities vector and the trace of pitch cone	°
χ^X	relative stress drop in notch root	mm^{-1}
$\chi_T{}^X$	relative stress drop in notch root of standardized test gear	mm^{-1}
Σ	shaft angle	°

Table 2 — General subscripts in ISO 10300 (all parts)

Subscripts	Description
0	tool
1	pinion
2	wheel
A, B, B1, B2, C	value according to method A, B, B1, B2 or C
D	Drive flank
C	Coast flank
T	relative to standardized test gear dimensions
(1), (2)	trials of interpolation

5 Application

5.1 Calculation methods

5.1.1 General

ISO 10300 (all parts) provides the procedures to predict load capacity of bevel gears. The most valid method is full-scale and full-load testing of a specific gear set design. However, at the design stage or in certain fields of application, some calculation methods are needed to predict load capacity. Therefore, methods A, B and C are used in this part of ISO 10300, while method A, if its accuracy and reliability are proven, is preferred over method B, which in turn is preferred over method C.

ISO 10300 (all parts) allows the use of mixed factor rating methods within method B1 or method B2. For example: method B for dynamic factor $K_{v\text{-}B}$ can be used with method C face load factor $K_{H\beta\text{-}C}$.

5.1.2 Method A

Where sufficient experience from the operation of other, similar designs is available, satisfactory guidance can be obtained by the extrapolation of the associated test results or field data. The factors involved in this extrapolation may be evaluated by the precise measurement and comprehensive mathematical analysis of the transmission system under consideration, or from field experience. All gear and load data are required to be known for the use of this method, which shall be clearly described and presented with all mathematical and test premises, boundary conditions and any specific characteristics of the method that influence the result. The accuracy and the reliability of the method shall be demonstrated. Precision, for example, shall be demonstrated through comparison with other, acknowledged gear measurements. The method should be approved by both the customer and the supplier.

5.1.3 Method B

Method B provides the calculation formulae to predict load capacity of bevel gears for which the essential data are known. However, sufficient experience from the operation of other, similar designs is needed in the evaluation of certain factors even in this method. The validity of these evaluations for the given operating conditions shall be checked.

5.1.4 Method C

Where suitable test results or field experience from similar designs, are unavailable for use in the evaluation of certain factors, a further simplified calculation method, method C, should be used.

5.2 Safety factors

The allowable probability of failure shall be carefully weighed when choosing a safety factor, in balancing reliability against cost. If the performance of the gears can be accurately appraised by testing the unit itself under actual load conditions, lower safety factors may be permitted. The safety factors shall be determined by dividing the calculated permissible stress by the specific evaluated operating stress.

In addition to this general requirement, and the special requirements relating to surface durability (pitting) and tooth root strength (see ISO 10300-2 and ISO 10300-3, respectively), safety factors shall be determined only after careful consideration of the reliability of the material data and of the load values used for calculation. The allowable stress numbers used for calculation are valid for a given probability of failure, or damage (the material values in ISO 6336-5, for example, are valid for a 1 % probability of damage), the risk of damage being reduced as the safety factors are increased, and vice versa. If loads, or the response of the system to vibration, are estimated rather than measured, a larger factor of safety should be used.

The following variations shall also be taken into consideration in the determination of a safety factor:

— variations in gear geometry due to manufacturing tolerances;

— variations in alignment of gear members;

— variations in material due to process variations in chemistry, cleanliness and microstructure (material quality and heat treatment);

— variations in lubrication and its maintenance over the service life of the gears.

The appropriateness of the safety factors will thus depend on the reliability of the assumptions, such as those related to load, on which the calculations are based, as well as on the reliability required of the gears themselves, in respect of the possible consequences of any damage that might occur in the case of failure.

Supplied gears or assembled gear drives should have a minimum safety factor for contact stress $S_{H,min}$ of 1,0. The minimum bending stress value $S_{F,min}$ should be 1,3 for spiral bevel including hypoid gears, and 1,5 for straight bevel gears or those with $\beta_m \leq 5°$.

The minimum safety factors against pitting damage and tooth breakage should be agreed between the supplier and customer.

5.3 Rating factors

5.3.1 Testing

The most effective overall approach to gear system performance management is through the full-scale, full-load testing of a proposed new design. Alternatively, where sufficient experience of similar designs exists and results are available, a satisfactory solution can be obtained through extrapolation from such data. On the other hand, where suitable test results or field data are not available, rating factor values should be chosen conservatively.

5.3.2 Manufacturing tolerances

Rating factors should be evaluated based on the minimum acceptable quality limits of the expected variation of component parts in the manufacturing process. The accuracy grade, B, shall preferably be determined as specified in ISO 17485, e.g. single pitch deviation for calculating the dynamic factor $K_{v\text{-}B}$.

5.3.3 Implied accuracy

Where the empirical values for rating factors are given by curves, this part of ISO 10300 provides curve fitting equations to facilitate computer programming.

NOTE The constants and coefficients used in curve fitting often have significant digits in excess of those implied by the reliability of the empirical data.

5.4 Further factors to be considered

5.4.1 General

In addition to the factors considered that influence pitting resistance and bending strength, other, interrelated system factors can have an important effect on overall transmission performance. Their possible effect on the calculations should be considered.

5.4.2 Lubrication

The ratings determined by the formulae of ISO 10300-2 and ISO 10300-3 shall be valid only if the gear teeth are operated with a lubricant of proper viscosity and additive package for the load, speed, and surface finish, and if there is a sufficient quantity of lubricant on the gear teeth and bearings to lubricate and maintain an acceptable operating temperature.

5.4.3 Misalignment

Many gear systems depend on external supports such as machinery foundations to maintain alignment of the gear mesh. If these supports are poorly designed, initially misaligned, or become misaligned during operation due to elastic or thermal deflections or other influences, overall gear system performance will be adversely affected.

5.4.4 Deflection

Deflection of gear supporting housings, shafts, and bearings due to external overhung, transverse, and thrust loads affects tooth contact across the mesh. Since deflection varies with load, it is difficult to obtain good tooth contact at different loads. Generally, deflection due to external loads from driven and driving equipment reduces capacity, and this, as well as deflection caused by internal forces, should be taken into account when determining the actual gear tooth contact.

5.4.5 Materials and metallurgy

Most bevel gears are made from case-hardened steel. Allowable stress numbers for this and other materials shall be taken preferably from ISO 6336-5 because these are determined by a multitude of tests on spur gears for which the material strains can be calculated very precisely. Additionally, different modes of steel making and heat treatment are considered in ISO 6336-5. Hardness and tensile strength as well as the quality grade shall also be criteria for choosing permissible stress numbers.

NOTE Higher quality steel grades indicate higher allowable stress numbers, while lower quality grades indicate lower allowable stress numbers (see ISO 6336-5).

5.4.6 Residual stress

Any ferrous material having a case core relationship is likely to have residual stress. If properly managed, such stress will be compressive at the tooth surface, thereby enhancing the bending fatigue strength of the gear tooth. Shot peening, case carburizing and induction hardening, if properly performed, are common methods of inducing compressive pre-stress in the surface of the gear teeth. Improper grinding techniques after heat treatment might reduce the residual compressive stresses or even introduce residual tensile stresses in the root fillets of the teeth, thereby lowering the allowable stress numbers.

5.4.7 System dynamics

The method of analysis used in this part of ISO 10300 includes a dynamic factor, K_v, which derates the gears for increased loads caused by gear tooth inaccuracies. Generally speaking, this provides simplified values for easy application.

The dynamic response of the system results in additional gear tooth loads, due to the relative motions of the connected masses of the driver and the driven equipment. The application factor, K_A, is intended to account for the operating characteristics of the driving and driven equipment. It should be recognized, however, that if the operating roughness of the drive, gearbox or driven equipment causes excitation with a frequency that is near one of the system's major natural frequencies, resonant vibrations can cause severe overloads possibly several times higher than the nominal load. Therefore, where critical service applications are concerned, performance of a vibration analysis of the complete system is recommended. This analysis shall comprise the total system, including driver, gearbox, driven equipment, couplings, mounting conditions and sources of excitation. Natural frequencies, mode shapes and the dynamic response amplitudes should be calculated.

5.4.8 Contact pattern

The teeth of most bevel gears are crowned in both their profile and lengthwise directions during the manufacturing process in order to allow for deflection of the shafts and mountings. This crowning results in a localized contact pattern during roll testing under light loads. Under design load, unless otherwise specified, the tooth contact pattern is spread over the tooth flank without concentrations of the pattern at the edges of either gear member.

The application of the rating formulae to bevel gears manufactured under conditions in which this process has not been carried out and which do not have an adequate contact pattern, may require modifications of the factors given in this part of ISO 10300. Such gears are not covered by ISO 10300 (all parts).

NOTE The total load used for contact pattern analysis can include the effects of an application factor (see Annex D for a fuller explanation of tooth contact development).

5.4.9 Corrosion

Corrosion of the gear tooth surface can have a significant detrimental effect on the bending strength and pitting resistance of the teeth. However, the quantification of the effect of corrosion on gear teeth is beyond the range of ISO 10300 (all parts).

5.5 Further influence factors in the basic formulae

The basic formulae presented in ISO 10300-2 and ISO 10300-3 include factors reflecting gear geometry or being established by convention, which need to be calculated in accordance with their formulae.

In the formulae in ISO 10300 (all parts), there are also factors that reflect the effects of variations in processing or the operating cycle of the unit. These are known as influence factors because they account for a number of influences. Although treated as independent, they might nevertheless affect each other to an extent that is beyond evaluation. They include the load factors, K_A, K_v, $K_{H\beta}$, $K_{F\beta}$, $K_{H\alpha}$ and $K_{F\alpha}$, as well as those factors influencing permissible stresses.

There are various methods of calculation to determine the influence factors. These are qualified, as needed, by the addition of subscripts A to C to the symbols. Unless otherwise specified (for example in an application standard), the more accurate method should be used for important transmissions. It is recommended that supplementary subscripts be used whenever the method used for evaluation of a factor would not otherwise be readily identifiable.

For some applications, it might be necessary to choose between factors determined by using alternative methods (for example, alternatives for the determination of the dynamic factor or the transverse load factor). When reporting the calculation, the method used should be indicated by extending the subscript.

EXAMPLE $K_{v\text{-}C}$, $K_{H\alpha\text{-}B}$

6 External force and application factor, K_A

6.1 Nominal tangential force, torque, power

For the purposes of ISO 10300 (all parts), pinion torque is used in the basic stress calculation formulae. In order to determine the bending moment on the tooth, or the force on the tooth surface, the tangential force is calculated, at the reference cone at mid-face width, as follows:

Nominal tangential force of bevel gears, F_{mt}:

$$F_{mt1,2} = \frac{2\,000\,T_{1,2}}{d_{m1,2}} \tag{1}$$

Nominal tangential force of virtual cylindrical gears, F_{vmt}:

$$F_{vmt} = F_{mt1} \frac{\cos \beta_v}{\cos \beta_{m1}} \tag{2}$$

Nominal torque of pinion and wheel, T:

$$T_{1,2} = \frac{F_{mt\,1,2}\,d_{m1,2}}{2\,000} = \frac{1\,000\,P}{\omega_{1,2}} = \frac{9\,549\,P}{n_{1,2}} \tag{3}$$

Nominal power, P:

$$P = \frac{F_{mt\,1,2}\,v_{mt\,1,2}}{1\,000} = \frac{T_{1,2}\,\omega_{1,2}}{1\,000} = \frac{T_{1,2}\,n_{1,2}}{9\,549} \tag{4}$$

Nominal tangential speed at mean point, v_{mt}:

$$v_{mt\,1,2} = \frac{d_{m\,1,2}\,\omega_{1,2}}{2\,000} = \frac{d_{m\,1,2}\,n_{1,2}}{19\,098} \tag{5}$$

The nominal torque of the driven machine is decisive. This is the operating torque to be transmitted over a long period of time and under the most severe, regular operating conditions.

The nominal torque of the driving machine may be used if it corresponds to the required torque of the driven machine.

6.2 Variable load conditions

If the load is not uniform, a careful analysis of the gear loads should be carried out, in which the external and internal factors are considered. It is recommended that all the different loads that occur during the anticipated life of the gears, and the duration of each load, are determined. A method based on Miner's Rule (see ISO 6336-6[3]) shall be used for determining the equivalent life of the gears for the torque spectrum.

6.3 Application factor, K_A

6.3.1 Application factor —General

In cases where no reliable experiences, or load spectra determined by practical measurement or comprehensive system analysis, are available, the calculation should use the nominal tangential force F_{mt} according to 6.1 and an application factor, K_A. This application factor makes allowance for any externally applied dynamic loads in excess of the nominal operating pinion torque, T_1.

6.3.2 Influences affecting external dynamic loads

In determining the application factor, account should be taken of the fact that many prime movers develop momentary peak torques considerably greater than those determined by the nominal ratings of either the prime mover or of the driven equipment. There are many possible sources of dynamic overload which should be considered, including:

— system vibration;

— critical speed;

— acceleration torques;

— overspeed;

— sudden variations in system operation;

— braking;

— negative torques, such as those produced by retarders on vehicles, which result in loading the reverse flanks of the gear teeth.

Analysis for critical speeds within the operating range of the drive train is essential. If critical speeds are present, changes in the design of the overall drive system shall be made in order to either eliminate them or provide system damping to minimize gear and shaft vibrations.

6.3.3 Establishment of application factors

Application factors are best established by a thorough analysis of service experience with a particular application. For applications such as marine gears, which are subjected to cyclic peak torques (torsional vibrations) and are designed for infinite life, the application factor can be defined as the ratio between cyclic peak torque and the nominal rated torque. The nominal rated torque is defined by the rated power and speed.

If the gear is subjected to a limited number of loads in excess of the amount of cyclic peak torque, this influence may be covered directly by means of cumulative fatigue analysis or by means of an increased application factor representing the influence of the load spectrum.

If service experience is unavailable, a thorough analytical investigation should be carried out. Annex C provides approximate values of K_A if neither of these alternatives is possible.

7 Dynamic factor, K_v

7.1 General

The dynamic factor, K_v, makes allowance for the effects of gear tooth quality related to speed and load as well as for the other parameters listed below (see 7.2 to 7.6). The dynamic factor relates the total tooth load, including internal dynamic effects, to the transmitted tangential tooth load and is expressed as the sum of the internal effected dynamic load and the transmitted tangential tooth load, divided by the transmitted tangential tooth load. The parameters for the gear tooth internal dynamic load fall into two categories: design and manufacturing.

7.2 Design

The design parameters include:

— pitch line velocity;

— tooth load;

— inertia and stiffness of the rotating elements;

— tooth stiffness variation;

— lubricant properties;

— stiffness of bearings and case structure;

— critical speeds and internal vibration within the gear itself.

7.3 Manufacturing

The manufacturing parameters include:

— tooth spacing variations;

— runout of pitch surfaces with respect to the axis of rotation;

— tooth flank variations;

— compatibility of mating gear tooth elements;

— balance of parts;

— bearing fit and preload.

7.4 Transmission error

Even if the input torque and speed are constant, significant vibration of the gear masses and the resultant dynamic tooth forces can exist. These forces result from the relative displacements between the mating gears as they vibrate in response to an excitation known as transmission error. The ideal kinematics of a gear pair require a constant ratio between the input and output. Transmission error is defined as the deviation from uniform relative angular motion of the pair of meshing gears. It is influenced by all deviations from the ideal gear tooth form of the actual gear design, the manufacturing procedure and the operational conditions. The operational conditions include the following:

a) pitch line velocity: the frequencies of the excitation depend on the pitch line velocity and module.

b) gear mesh stiffness variations: as the gear teeth pass through the meshing cycle, gear mesh stiffness variations are a source of excitation especially pronounced in straight and Zerol bevel gears. Spiral bevel gears with a total contact ratio > 2 have less stiffness variation;

c) transmitted tooth load: since deflections are load dependent, gear tooth profile modifications can be designed to give uniform velocity ratio only for one load magnitude. Loads different from the design load increase the transmission error;

d) dynamic unbalance of the gears and shafts;

e) application environment: excessive wear and plastic deformation of the gear tooth profiles increase the transmission error. Gears shall have a properly designed lubrication system, enclosure, and seals to maintain a safe operating temperature and an environment free of contamination;

f) shaft alignment: gear tooth alignment is influenced by load and thermal deformations of gears, shafts, bearings and housings;

g) tooth friction induced excitation.

7.5 Dynamic response

The effects of dynamic tooth forces are influenced by the following:

— mass of the gears, shafts, and other major internal components;

— stiffness of the gear teeth, gear blanks, shafts, bearings and housings;

— damping, of which the principal sources are the shaft bearings and seals, with other sources including the hysteresis of the gear shafts, viscous damping at sliding interfaces and couplings.

7.6 Resonance

7.6.1 General

When an excitation frequency (tooth meshing frequency, multiples of tooth meshing frequencies, etc.) coincides, or nearly coincides, with a natural frequency of the gearing system, a resonant vibration can cause high dynamic tooth loading. When the magnitude of internal dynamic load at such a driving speed becomes large, operation in this speed range should be avoided.

7.6.2 Gear blank resonance

The gear blanks of high-speed or lightweight gearing can have natural frequencies within the operating speed range. If the gear blank is excited by a frequency close to one of its natural frequencies, the resonant deflections might cause high dynamic tooth loads. There is also the possibility of plate or shell mode vibrations which can cause the gear blank to fail. If determined by method B or C, the dynamic factor, K_v, does not account for gear blank resonance.

7.6.3 System resonance

The gearbox is just one component of a system comprising power source, gearbox, driven equipment and interconnecting shafts and couplings. The dynamic response of this system depends on its configuration. In certain cases, a system can possess a natural frequency close to the excitation frequency associated with an operating speed. Under such resonant conditions, its operation shall be carefully evaluated. For critical drives, a detailed analysis of the entire system is recommended. This should then be taken into account when determining the effects on the application factor.

7.7 Calculation methods for K_v

7.7.1 General comments

A bevel gear drive is a very complicated vibration system. The dynamic system as well as the natural frequencies which induce dynamic tooth loading cannot be determined by consideration of the pair of gears alone. The pinion shaft alignment can change considerably depending on the craftsmanship of the assembly, the backlash and the elastic deformation of gear shafts, bearings or housing.

A slight change in alignment alters the relative rotation angle of the gearing and thus the dynamic loading on the gears. Crowning in the lengthwise and profile directions can preclude true conjugate action and make tooth accuracy difficult to determine.

Under such circumstances, reliable values of the dynamic factor, K_v, can best be predicted by a mathematical model which has been satisfactorily verified by test measurements. If the known dynamic loads are added to the nominal transmitted load, then the dynamic factor should be set to unity.

To determine K_v, several methods are indicated in descending order of precision, from method A ($K_{v\text{-}A}$) to method C ($K_{v\text{-}C}$).

When using method B or C for hypoid gears which have a "typical" amount of hypoid offset, the dynamic factor is assumed to have the value 1 because of the damping properties of the sliding conditions in mesh. For smaller amounts of offset, the dynamic factor is interpolated between the value calculated as for bevel gears without offset and the value 1. The lower limit of a typical offset value is assumed to be 5 % of the mean pitch diameter of the wheel (a_{rel} = 0,1); for the upper limit, see ISO 23509.

Dynamic factor, K_v:

$$K_v = K_v^* - \frac{K_v^* - 1}{0{,}1} a_{rel} \geq 1 \tag{6}$$

with $K_v^* = K_{v\text{-}B}$ according to 7.7.3 or $K_v^* = K_{v\text{-}C}$ according to 7.7.4;

$$a_{rel} = \frac{2\,|a|}{d_{m2}} \tag{7}$$

7.7.2 Method A, $K_{v\text{-}A}$

$K_{v\text{-}A}$ is determined by a comprehensive analysis, confirmed by experience of similar designs, using the following general procedures:

a) a mathematical model of the vibration system is developed which refers to the entire power transmission, including the gearbox;

b) the transmission error of the bevel gears under load is measured, or calculated by a reliable simulation programme for transmission error of bevel gears;

c) the dynamic load response of the pinion and gear shafts is analysed with the system model, a), excited by the transmission error, b).

7.7.3 Method B, $K_{v\text{-}B}$

7.7.3.1 General

This method makes the simplifying assumption that the gear pair constitutes an elementary single mass and spring system comprising the combined masses of pinion and wheel, with a spring stiffness being the mesh stiffness of the contacting teeth. In accordance with this assumption, forces due to torsional vibrations of the shafts and coupled masses are not covered by $K_{v\text{-}B}$. This is realistic if other masses (apart from the gear pair) are connected by shafts of relatively low torsional stiffness. For bevel gears with significant lateral shaft flexibility, the real natural frequency will be less than calculated.

The amount of the dynamic overloads is, among other effects, a function of the accuracy of the gear, i.e. the flank form and pitch deviations. The flank form deviation of bevel gears is not as easy to measure as an involute form of cylindrical gears (see ISO/TR 10064-6[4]), and ISO tolerances do not exist. However, single flank composite tolerances are specified in ISO 17485 and the transmission error of a bevel gear set should be checked accordingly if proper equipment is available. On the other hand, the pitch deviations can be measured relatively easily. So, in these cases, the simplifying assumption is made that the single pitch deviation is a representative value of the transmission error for determination of the dynamic factor.

The following data are needed for the calculation of $K_{v\text{-}B}$:

a) accuracy of gear pair (single pitch deviation as specified in ISO 17485);

b) mass moment of inertia of pinion and wheel (dimensions and material density);

c) tooth stiffness;

d) transmitted tangential load.

7.7.3.2 Speed ranges

Dimensionless reference speed:

$$N = \frac{n_1}{n_{E1}} \tag{8}$$

where n_{E1} is the resonance speed according to 7.7.3.3.

With the aid of the reference speed, N, the total speed range can be subdivided into four sections: subcritical, main resonance, supercritical and an intermediate sector (main resonance/supercritical).

Because of the influence of stiffness values which are not included (for example those of shafts, bearings, gearbox), and because of the damping, the resonance speed can be above or below the speed calculated with Formula (9). For reasons of safety, a resonance sector of $0{,}75 < N \le 1{,}25$ is defined.

This results in the cited sectors for the calculation of $K_{v\text{-}B}$:

— subcritical sector, $N \le 0{,}75$, determined by method A or B;

— main resonance sector, $0{,}75 < N \le 1{,}25$, operation in this sector should be avoided, but if unavoidable, refined analysis by method A shall be carried out;

— intermediate sector, $1{,}25 < N < 1{,}5$, determined by method A or B;

— supercritical sector, $N \ge 1{,}5$, determined by method A or B.

See ISO 6336-1[2] for further information on the speed ranges.

7.7.3.3 Resonance speed

Resonance speed of pinion:

$$n_{E1} = \frac{30 \times 10^3}{\pi\, z_1} \sqrt{\frac{c_\gamma}{m_{red}}} \tag{9}$$

where

c_γ is the mean value of mesh stiffness [see Formula (11)]:

$$m_{red} = \frac{m_1^* m_2^*}{m_1^* + m_2^*} \tag{10}$$

m_{red} is the mass per millimetre face width reduced to the line of action of the dynamically equivalent cylindrical gear pair.

A value of $c_{\gamma 0}$ = 20 N/(mm·µm) applies to spur gears. Investigations of helical gears have shown that the stiffness decreases with increasing helix angles. On the other hand, the spiral arrangement of bevel gear teeth around a conical blank leads to higher rigidity of bevel gears, except straight bevel gears. Therefore, due to the lack of any better knowledge, the stiffness for a spur gear is assumed to be suitable for bevel gears in average conditions which are given by $F_{vmt}\, K_A / b_{v,eff} \ge 100$ N/mm and $b_{v,eff}/b_v \ge 0{,}85$.

The mean value of mesh stiffness per unit face width, c_γ, is determined by:

$$c_\gamma = c_{\gamma 0} C_F \tag{11}$$

where

$c_{\gamma 0}$ is mesh stiffness for average conditions; a value of 20 N/(mm·μm) is recommended.

C_F is a correction factor for non-average conditions:

a) for $F_{vmt} K_A / b_{v,eff} \geq 100$ N/mm $\qquad C_F = 1$ (12a)

b) for $F_{vmt} K_A / b_{v,eff} < 100$ N/mm $\qquad C_F = (F_{vmt} K_A / b_{v,eff})/100$ N/mm (12b)

$b_{v,eff}$ is effective face width of the virtual cylindrical gear. The effective face width $b_{v,eff}$ is the real length of contact pattern (see Annex D). In the case of full load, the contact pattern typically has a minimum length of 85 % of face width b_v. If it is not possible to obtain information of contact pattern length under load conditions, $b_{v,eff} = 0{,}85\, b_v$ should be used.

If an exact determination of the mass moments of inertia m_1^* and m_2^* of the bevel gears is either not feasible due to cost or otherwise impossible (for example, at the design stage), bevel gears of common gear blank design should be replaced by approximate dynamically equivalent cylindrical gears (suffix x) (see Figure 2).

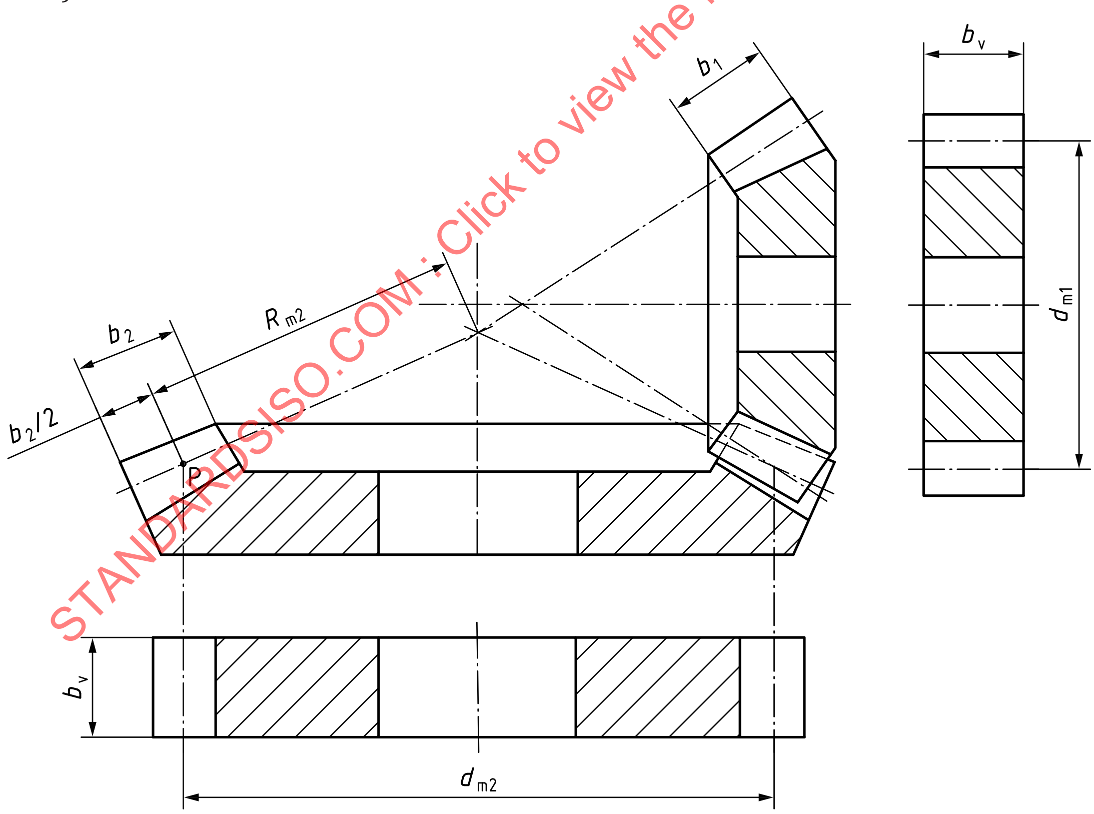

Figure 2 — Approximate dynamically equivalent cylindrical gears for the determination of the dynamic factor of bevel gears including hypoid gears

Relative gear mass per unit face width reduced to the line of action:

$$m_{1,2}^{*} \approx m_{1x,2x}^{*} = \frac{1}{8}\rho\ \pi\ \frac{d_{m1,2}^{2}}{\cos^{2}\left[\left(\alpha_{nD}+\alpha_{nC}\right)/2\right]} \tag{13}$$

where ρ is the density of the gear material (for steel ρ = 7,86·10^{-6} kg/mm^3)

See Figure 3 for the graphical determination of resonance speed for the mating solid steel pinion/solid wheel (bevel gears without offset only).

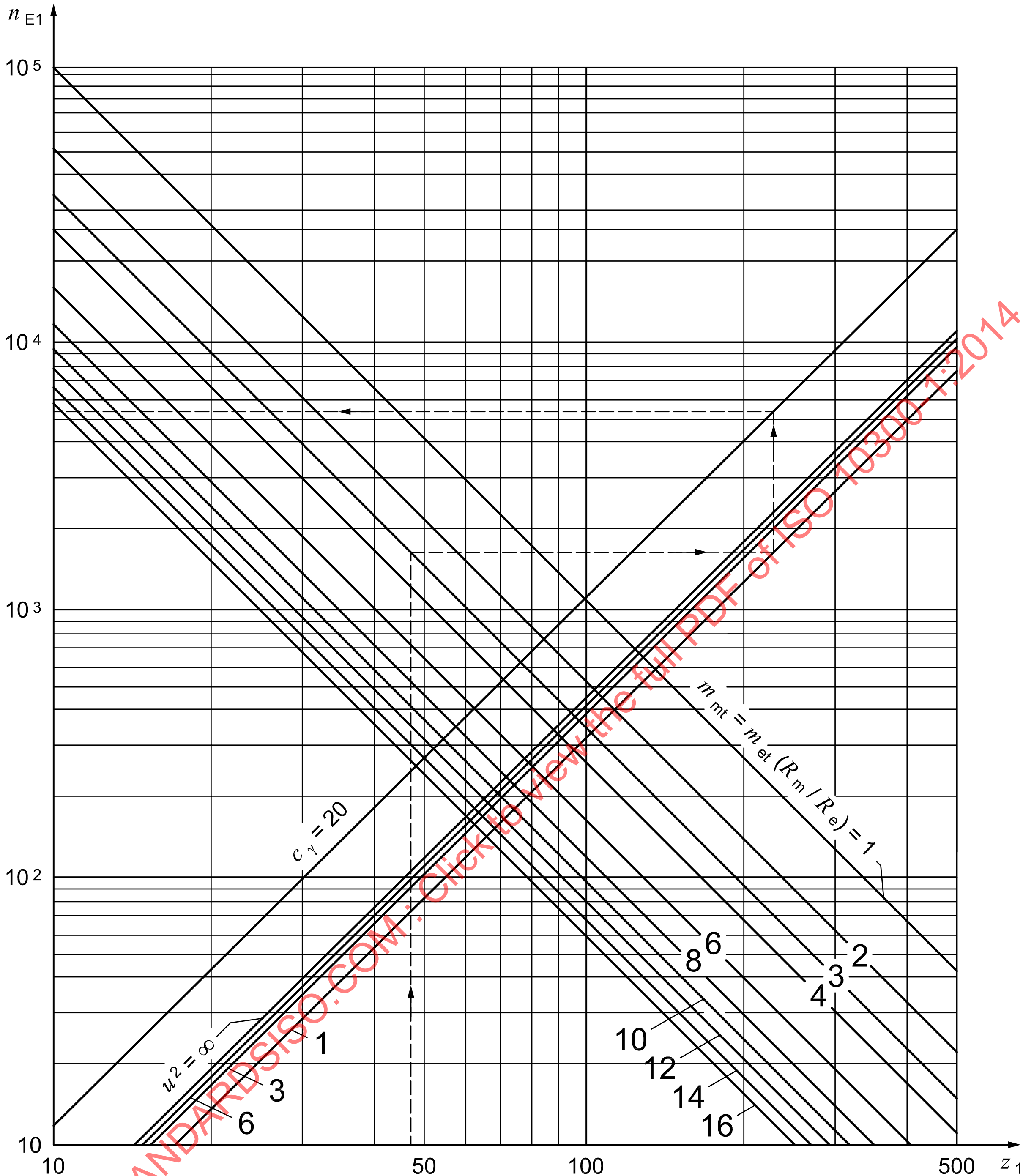

Key

z_1 number of pinion teeth (—)

n_{E1} resonance speed (min^{-1})

Figure 3 — Nomogram for the determination of the resonance speed, n_{E1}, for the mating solid steel pinion/solid wheel, with c_γ = 20 N/(mm · µm) (for bevel gears without offset only)

7.7.3.4 Subcritical sector ($N \leq 0,75$)

Common operating range for industrial and vehicle gears:

$$K_{\text{v-B}} = N \cdot K + 1 \tag{14}$$

With the simplifying assumptions given in 7.7.3.1, Formula (15) applies:

$$K = \frac{b_{\text{v}}\, f_{\text{p,eff}}\, c'}{F_{\text{vmt}}\, K_{\text{A}}} c_{\text{v1,2}} + c_{\text{v3}} \tag{15}$$

where

$$f_{\text{p,eff}} = f_{\text{pt}} - y_{\text{p}} \text{ with } y_{\text{p}} \approx y_{\text{a}} \tag{16}$$

See Formula (17) for c'; Table 3 for $c_{\text{v1,2}}$ and c_{v3}; see 9.3.1 for f_{pt} and 9.5 for y_{a}.

NOTE Any positive influence of tip relief or profile crowning is not considered. The calculation is, therefore, on the safe side for bevel gears which normally have profile crowning.

Table 3 — Influence factors c_{v1} to c_{v7} in Formulae (15) to (19)

Influence factor	$1 < \varepsilon_{\text{v}\gamma} \leq 2$[a]	$\varepsilon_{\text{v}\gamma} > 2$[a]	–
c_{v1}[b]	0,32	0,32	$c_{\text{v1,2}} = c_{\text{v1}} + c_{\text{v2}}$
c_{v2}[c]	0,34	$\dfrac{0,57}{\varepsilon_{\text{v}\gamma} - 0,3}$	
c_{v3}[d]	0,23	$\dfrac{0,096}{\varepsilon_{\text{v}\gamma} - 1,56}$	
c_{v4}[e]	0,90	$\dfrac{0,57 - 0,05\varepsilon_{\text{v}\gamma}}{\varepsilon_{\text{v}\gamma} - 1,44}$	
c_{v5}[f]	0,47	0,47	$c_{\text{v5,6}} = c_{\text{v5}} + c_{\text{v6}}$
c_{v6}[f]	0,47	$\dfrac{0,12}{\varepsilon_{\text{v}\gamma} - 1,74}$	
–	$1 < \varepsilon_{\text{v}\gamma} \leq 1,5$	$1,5 < \varepsilon_{\text{v}\gamma} \leq 2,5$	$\varepsilon_{\text{v}\gamma} > 2,5$
c_{v7}[g]	0,75	$0,125 \sin[\pi(\varepsilon_{\text{v}\gamma} - 2)] + 0,875$	1,0

[a] For $\varepsilon_{\text{v}\gamma}$, see Formula (A.25) according to method B1 or Formula (B.23) according to method B2.

[b] This influence factor allows for pitch deviation effects and is assumed to be constant.

[c] This influence factor allows for tooth profile deviation effects.

[d] This influence factor allows for the cyclic variation effect in mesh stiffness.

[e] This influence factor takes into account resonant torsional oscillations of the gear pair, excited by cyclic variation of the mesh stiffness.

[f] In the supercritical sector the influences on $K_{\text{v-B}}$ of the influence factors c_{v5} and c_{v6} correspond to those of c_{v1} and c_{v2} in the subcritical sector;

[g] This influence factor takes into account the component of force which, due to mesh stiffness variation, is derived from tooth bending deflections during substantially constant speed.

A value of c_0' = 14 N/(mm·µm) applies to spur gears. Investigations of helical gears have shown that the tooth stiffness decreases with increasing helix angles. On the other hand, the spiral arrangement of bevel gear teeth around a conical blank leads to higher rigidity of bevel gears, except straight bevel gears. Therefore, due to the lack of any better knowledge, the tooth stiffness for a spur gear is assumed to be suitable for bevel gears in average conditions which are given by $F_{vmt}\, K_A/b_{v,eff} \geq 100$ N/mm and $b_{v,eff}/b_v \geq 0{,}85$.

The single stiffness, c', see ISO 6336-1,[2] is determined as follows:

$$c' = c'_0 C_F \tag{17}$$

where

c_0' is single stiffness for average conditions, a value of 14 N/(mm·µm) is recommended;

C_F is a correction factor for non-average conditions [see Formulae (12a) and (12b)].

7.7.3.5 Main resonance sector (0,75 < N ≤ 1,25)

With the simplifying assumptions given in 7.7.3.1, Formula (18) applies:

$$K_{v-B} = \frac{b_v\, f_{p,eff}\, c'}{F_{vmt}\, K_A} c_{v1,2} + c_{v4} + 1 \tag{18}$$

For $c_{v1,2}$ and c_{v4} see Table 3.

7.7.3.6 Supercritical sector (N ≥ 1,5)

High-speed gears and those with similar requirements operate in the supercritical sector:

$$K_{v-B} = \frac{b_v\, f_{p,eff}\, c'}{F_{vmt}\, K_A} c_{v5,6} + c_{v7} + 1 \tag{19}$$

For c' and $f_{p,eff}$ see 7.7.3.3; for $c_{v5,6}$ and c_{v7} see Table 3.

7.7.3.7 Intermediate sector (1,25 < N < 1,5)

In the intermediate sector, the dynamic factor is determined by linear interpolation between K_{v-B} at N = 1,25 and K_{v-B} at N = 1,5. K_{v-B} is calculated according to 7.7.3.4 and 7.7.3.5, respectively:

$$K_{v-B} = K_{v-B\,(N\,=\,1,5)} + \frac{K_{v-B\,(N\,=\,1,25)} - K_{v-B\,(N\,=\,1,5)}}{0{,}25} (1{,}5 - N) \tag{20}$$

7.7.4 Method C, K_{v-C}

7.7.4.1 General comments

Figure 4 shows dynamic factors which should be used in the absence of specific knowledge of the dynamic loads. The curves of Figure 4 and the equations given in 7.7.4.3 [i.e. Formulae (21) to (26)] are based on empirical data, and do not account for resonance (see 7.6).

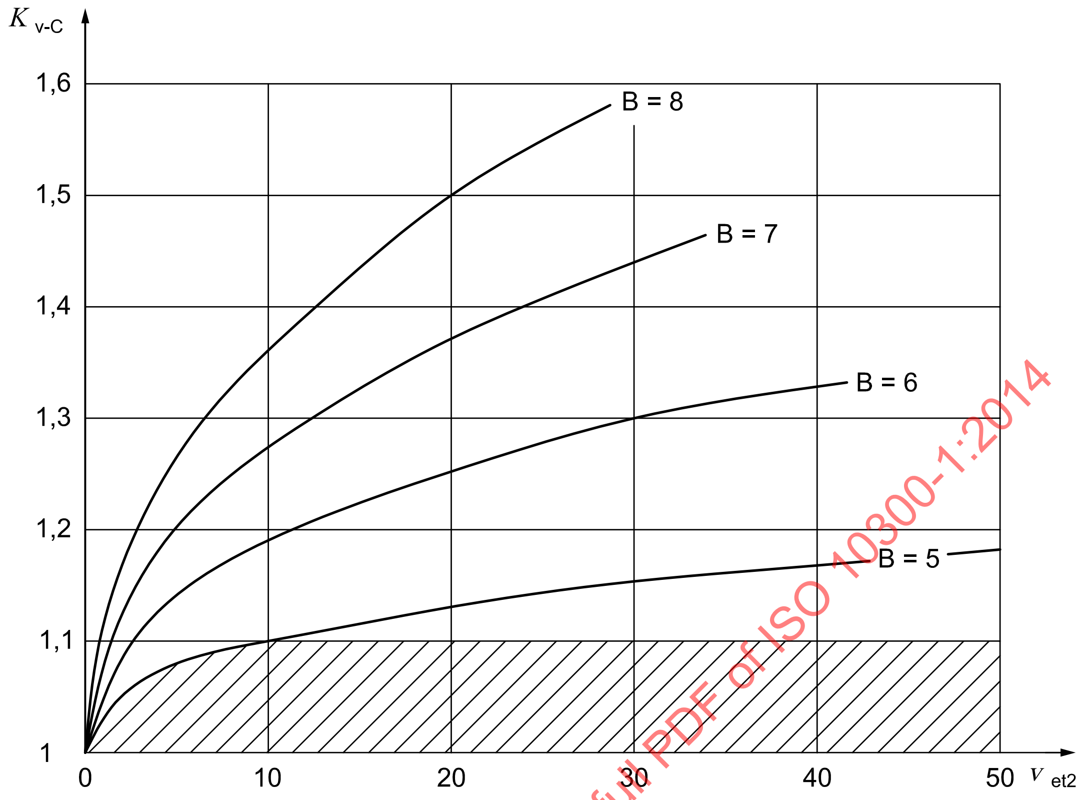

Key

v_{et2} wheel pitch line velocity at the outer pitch diameter (m/s)

$K_{v\text{-}C}$ dynamic factors

B accuracy grade according to Formula (25)

NOTE The hatched area stands for "very accurate gearing".

Figure 4 — Dynamic factor, $K_{v\text{-}C}$

Because of the approximate nature of the empirical curves, and the lack of measured tolerance values at the design stage, the dynamic factor curve should be selected based on experience of manufacturing methods and taking into account the operating conditions affecting the design (see 7.7.1). In most cases, the contact pattern on the tooth flank is helpful for comparison with previous experience.

The choice of curves B = 5 to B = 8 and "very accurate gearing" (7.7.4.2), should be based on the transmission error (see 7.4). If transmission error is not available, it is reasonable to refer to the contact pattern on the tooth flank. If the contact pattern on each tooth flank is not uniform, pitch accuracy (single pitch deviation) can be incorporated as a representative value to determine the dynamic factor.

7.7.4.2 Very accurate gearing

Where gearing is manufactured using process control to very accurate gearing grades (generally speaking, when B < 5 in accordance with ISO 17485, or where design, manufacturing and application experience ensure a low transmission error), values of K_v between 1,0 and 1,1 may be used, depending on the specifier's experience with similar applications and the degree of accuracy actually achieved. In order to be able to use these values correctly, the gearing shall be maintained with accurate alignment and adequate lubrication so that its overall accuracy is maintained under the operating conditions.

7.7.4.3 Empirical curves

The empirical curves B = 5 to B = 8 shown in Figure 4 are generated with the following limitations for values of B, such that:

— $5 \le B \le 8$

— $6 \le z \le 1200$ or $(3000/m_{mn})$, whichever is less

— $1{,}25 \le m_{mn} \le 50$

Curves may be extrapolated beyond the end points shown in Figure 4 based on experience and careful consideration of the factors influencing dynamic load. For the purposes of computer calculations, Formula (26) defines the end points of the curves in Figure 4.

The dynamic factor, K_{v-C} is:

$$K_{v-C} = \left(\frac{A}{A + \sqrt{200\, v_{et2}}} \right)^{-X} \tag{21}$$

where

$$v_{et2} = v_{mt2} \frac{d_{e2}}{d_{m2}} \tag{22}$$

$$A = 50 + 56\,(1{,}0 - X); \tag{23}$$

$$X = 0{,}25\,(B - 4{,}0)^{0{,}667}; \tag{24}$$

B is the ISO accuracy grade as specified in ISO 17485, intended for the actual gear set.

The accuracy grade B may also be calculated with knowledge of the single pitch deviation:

$$B = 4 + 2{,}88\,539 \cdot \ln \left(\frac{f_{pt}}{0{,}003\, d_T + 0{,}3\, m_{mn} + 5} \right) \tag{25}$$

where

ln is the natural logarithmic function, i.e. $\log_e()$;

d_T is the tolerance diameter according to ISO 17485;

m_{mn} is the mean normal module;

f_{pt} is the single pitch deviation (at mean point), in micrometres.

The maximum recommended pitch line velocity, $v_{et2,max}$, for a given accuracy grade B is determined as follows:

$$v_{et2,max} = \frac{\left[A + (13 - B) \right]^2}{200} \tag{26}$$

where $v_{et2,max}$ is the maximum wheel pitch line velocity at the outer pitch diameter (end point of K_v curves in Figure 4), in metres per second.

8 Face load factors, $K_{H\beta}$, $K_{F\beta}$

8.1 General documents

8.1.1 The face load factors, $K_{H\beta}$ and $K_{F\beta}$, modify the rating formulae for the gear flank and for the tooth root to reflect the non-uniform distribution of the load along the face width.

8.1.2 $K_{H\beta}$ is defined as the ratio between the maximum load per unit face width and the mean load per unit face width.

8.1.3 $K_{F\beta}$ is defined as the ratio between the maximum tooth root stress and the mean tooth root stress along the face width.

8.1.4 The amount of non-uniform load distribution is influenced by:

— gear tooth manufacturing accuracy, and tooth contact pattern and spacing;

— alignment of the gears in their mountings;

— elastic deflections of the gear teeth, shafts, bearings, housings and foundations, which support the gear unit, resulting from either the internal or external gear loads;

— bearing clearances;

— Hertzian contact deformation of the tooth surfaces;

— thermal expansion and distortion of the gear unit due to operating temperatures (especially important on gear units where the gear housing is made from a different material than the gears, shafts and bearings);

— centrifugal deflections due to operating speeds.

8.1.5 The geometric characteristics of a bevel gear tooth change along its face width. Accordingly, the magnitudes of the axial and radial components of the tangential load vary with the position of the tooth contact. Similarly, the deflections of the mountings and of the tooth itself vary, and in turn affect the position of the tooth contact and its size and shape.

For applications in which the operating torque varies, the desired contact shall be considered “ideal” at full load only. For intermediate loads, a satisfactory compromise should be accepted.

Attention — ISO 10300 (all parts) is not applicable to bevel gears which have a poor contact pattern (see 5.4.8 and Annex D).

8.2 Method A

A comprehensive analysis of all influence factors, such as measurement of tooth root stress in service, is needed for an exact determination of the load distribution across the face width according to method A. However, due to its high cost, this type of analysis is generally restricted in practice.

8.3 Method B

A standardized approach for bevel gear face load factors corresponding to method B has not yet been developed. However, face load distribution can be determined on the basis of a loaded tooth contact analysis (LTCA) and should be used if available.

8.4 Method C

8.4.1 Face load factor, $K_{H\beta\text{-}C}$

In the case of bevel gears, the face load distribution is influenced essentially by the crowning of the gear teeth and by the deflections occurring in service. This is considered in the calculation of the length of the contact line (see Annex A) as well as in the calculation of the load distribution (see Figure 2 of ISO 10300-2:2014), which applies, however, only to gear sets with satisfactory contact patterns as defined in Annex D.

The influence of the deflections, and thus of the bearing arrangement, is accounted for by the mounting factor $K_{H\beta\text{-be}}$, according to Table 4.

The load distribution factor $K_{H\beta\text{-}C}$ is:

$$K_{H\beta\text{-C}} = 1{,}5\ K_{H\beta\text{-be}} \tag{27}$$

Attention — Formula (27) is not valid for uncrowned gears.

Table 4 — Mounting factor, $K_{H\beta\text{-be}}$

Verification of contact pattern	**Mounting conditions of pinion and wheel**		
Contact pattern is checked:	Neither member cantilever mounted	One member cantilever mounted	Both members cantilever mounted
for each gear set in its housing under full load	1,00	1,00	1,00
for each gear set under light test load	1,05	1,10	1,25
for a sample gear set and estimated for full load	1,20	1,32	1,50
NOTE Based on optimum tooth contact as evidenced by results of a contact pattern test on the gears in their mountings.			

WARNING — The observed contact pattern is normally an accumulated picture of each possible tooth pair combination. Formula (27) is valid only if the movement of the tooth contact pattern, during one revolution of the wheel, either towards the heel or toe, is small. Otherwise, the smallest contact pattern should be taken for the determination of $b_{v,eff}$. This movement of single contact patterns might be particularly pronounced for gears finished only by lapping.

8.4.2 Face load factor, $K_{F\beta\text{-}C}$

K_{Fb} accounts for the effect of the load distribution across the face width on the tooth root stress:

$$K_{F\beta\text{-C}} = K_{H\beta\text{-C}} / K_{F0} \tag{28}$$

For $K_{H\beta}$ see 8.4.1; K_{F0} see 8.4.3.

8.4.3 Lengthwise curvature factor for bending strength, K_{F0}

The lengthwise curvature factor K_{F0} considers the contact pattern shift under different loads which is smallest, if the lengthwise tooth curvature at the mean point corresponds to that of an involute curve. This effect is well known and depends on the cutter radius r_{c0} and the spiral angle β_{m2}.

The following are the two cases to be considered.

a) For straight and Zerol bevel gears as well as spiral bevel gears with large cutter radii ($r_{c0} > R_{m2}$):

$$K_{F0} = 1{,}0 \tag{29a}$$

b) For other spiral bevel and hypoid gears:

$$K_{F0} = 0{,}211 \left(\frac{\rho_{m\beta}}{R_{m2}} \right)^q + 0{,}789 \tag{29b}$$

where

$\rho_{m\beta}$ is the lengthwise tooth mean radius of curvature;

R_{m2} is mean cone distance of the wheel;

$$q = \frac{0{,}279}{\log_{10}(\sin\beta_{m2})} \tag{30}$$

The lengthwise tooth mean radius of curvature, $\rho_{m\beta}$, (see ISO 23509) is calculated as follows:

— for face milled gears:

$$\rho_{m\beta} = r_{c0} \tag{31a}$$

— for face hobbed gears:

$$\rho_{m\beta} = R_{m2}\cos\beta_{m2}\left[\tan\beta_{m2} + \frac{\tan\eta_1}{1+\tan\nu_0\,(\tan\beta_{m2}+\tan\eta_1)} \right] \tag{31b}$$

where

$$\nu_0 = \arcsin\left(\frac{m_{mn} z_0}{2\,r_{c0}} \right) \tag{32}$$

$$\eta_1 = \arccos\left(\frac{R_{m2}\cos\beta_{m2}}{\sqrt{R_{m2}^2 + r_{c0}^2 - 2\,R_{m2}\,r_{c0}\sin(\beta_{m2}-\nu_0)}} \left(1 + \frac{z_0}{z_2}\sin\delta_2 \right) \right) \tag{33}$$

The range of validity of face load factor, K_{F0}, is limited.

If the calculated value of $K_{F0} > 1{,}15$ set $K_{F0} = 1{,}15$; if the calculated value of $K_{F0} < 1{,}00$ set $K_{F0} = 1{,}0$.

9 Transverse load factors, $K_{H\alpha}$, $K_{F\alpha}$

9.1 General comments

The distribution of the total tangential force over several pairs of meshing teeth depends, in the case of given gear dimensions, on the gear accuracy and the amount of the total tangential force.

The factor $K_{H\alpha}$ accounts for the effect of the load distribution on the contact stress, while $K_{F\alpha}$ accounts for the effect of the load distribution on the tooth root stress (see ISO 6336-1[2] for further information). The use of method A requires comprehensive analysis (see 9.2), whereas the methods of approximation B and C (see 9.3 and 9.4) are sufficiently accurate in most cases.

When using methods B or C, the transverse load factors for gears with small offset are interpolated between the value for non-offset bevel gears and 1. The value 1 is assumed to be a realistic value for hypoid gears with a typical amount of offset (see 7.7.1) because the running-in effect adapts the flanks under load.

Transverse load factors, $K_{\mathrm{H\alpha}}$, $K_{\mathrm{F\alpha}}$:

$$K_{\mathrm{H\alpha}} = K_{\mathrm{F\alpha}} = K_{\mathrm{H\alpha}}^{*} - \frac{K_{\mathrm{H\alpha}}^{*} - 1}{0,1} a_{\mathrm{rel}} \geq 1 \tag{34}$$

with $K_{\mathrm{H\alpha}}^{*} = K_{\mathrm{H\alpha-B}}$ according to 9.3 or $K_{\mathrm{H\alpha}}^{*} = K_{\mathrm{H\alpha-C}}$ according to 9.4;

$$a_{\mathrm{rel}} = \frac{2\,|a|}{d_{\mathrm{m2}}} \tag{35}$$

9.2 Method A

The load distribution taken as the basis for the load capacity calculation should be determined by measurement or by an exact analysis of all influence factors. However, when the latter is used, the method's accuracy and reliability shall be proved and its premises clearly presented.

9.3 Method B

9.3.1 Bevel gears having virtual cylindrical gears with contact ratio $\varepsilon_{\mathrm{v\gamma}} \leq 2$

Transverse load factors, $K_{\mathrm{H\alpha}}$, $K_{\mathrm{F\alpha}}$:

$$K_{\mathrm{H\alpha}} = K_{\mathrm{F\alpha}} = \frac{\varepsilon_{\mathrm{v\gamma}}}{2}\left[0,9 + 0,4 \frac{c_{\gamma}\left(f_{\mathrm{pt}} - y_{\alpha}\right)}{F_{\mathrm{mtH}}/b_{\mathrm{v}}}\right] \tag{36}$$

where

c_{γ} is the mesh stiffness, as an approximation, c_{γ} = 20 N/(mm · µm) (see 7.7.3.3);

f_{pt} is the single pitch deviation, maximum value of pinion or wheel; for design calculations, the tolerance of the wheel according to ISO 17485 should be used;

y_{α} is the running-in allowance (see 9.5);

F_{mtH} is the determinant tangential force at mid-face width on the pitch cone:

$$F_{\mathrm{mtH}} = F_{\mathrm{vmt}} K_{\mathrm{A}} K_{\mathrm{v}} K_{\mathrm{H\beta}}. \tag{37}$$

$K_{\mathrm{H\alpha}}$, $K_{\mathrm{F\alpha}}$ may also be taken from Figure 5.

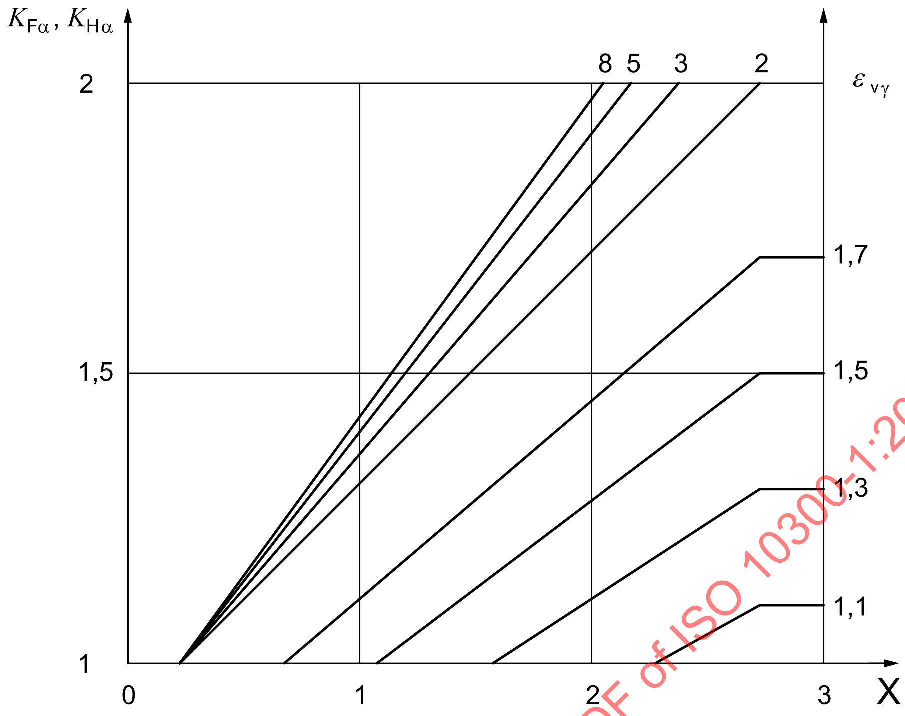

Key

X parameter for irregularity of transmission $\left[\frac{c_\gamma\left(f_{pt}-y_\alpha\right)}{F_{mtH}/b_v}\right]$

$K_{H\alpha}$ transverse load factor for contact stress

$K_{F\alpha}$ transverse load factor for bending stress

$\varepsilon_{v\gamma}$ virtual contact ratio (method B1), modified contact ratio (method B2)

Figure 5 — Transverse load factors, $K_{H\alpha\text{-B}}$ and $K_{F\alpha\text{-B}}$

9.3.2 Bevel gears having virtual cylindrical gears with contact ratio $\varepsilon_{v\gamma} > 2$

Transverse load factors, $K_{H\alpha}$, $K_{F\alpha}$:

$$K_{H\alpha}=K_{F\alpha}=0{,}9+0{,}4\sqrt{\frac{2\left(\varepsilon_{v\gamma}-1\right)}{\varepsilon_{v\gamma}}}\cdot\frac{c_\gamma\left(f_{pt}-y_\alpha\right)}{F_{mtH}/b_v} \tag{38}$$

for c_γ, f_{pt}, y_α, F_{mtH} see 9.3.1.

9.3.3 Boundary conditions

9.3.3.1 If the calculated value for $K_{H\alpha}$ exceeds one of both limits, $K_{H\alpha}$ is set to the respective limit value.

a) Method B1:

$$1 \le K_{H\alpha} \le \varepsilon_{v\gamma}\Big/\left(\varepsilon_{v\alpha}\, Z_{LS}^2\right) \tag{39a}$$

b) Method B2:

$$1 \leq K_{H\alpha} \leq \varepsilon_{v\gamma} / (\varepsilon_{v\alpha}\, \varepsilon_{NI}) \tag{39b}$$

with Z_{LS} as specified in 6.4.2 of ISO 10300-2:2014 and ε_{NI} as specified in 7.4.2.3 of ISO 10300-2:2014.

9.3.3.2 If the calculated value for $K_{F\alpha}$ exceeds one of both limits, $K_{F\alpha}$ is set to the respective limit value.

a) Method B1:

$$1 \leq K_{F\alpha} \leq \varepsilon_{v\gamma} / (\varepsilon_{v\alpha}\, Y_{LS}) \tag{40a}$$

b) Method B2:

$$1 \leq K_{F\alpha} \leq \varepsilon_{v\gamma} / (\varepsilon_{v\alpha}\, \varepsilon_{N}) \tag{40b}$$

with Y_{LS} as specified in 6.4.5 of ISO 10300-3:2014 and ε_N as specified in 7.4.4.3 and 7.4.5.2 of ISO 10300-3:2014.

With these boundary conditions, the most unfavourable load distribution is assumed, i.e. only one pair of teeth transmits the total tangential force, and the calculation is therefore on the safe side. It is recommended that the accuracy of bevel gears be chosen so that neither $K_{H\alpha}$ nor $K_{F\alpha}$ exceeds the value of $\varepsilon_{v\alpha n}$.

9.4 Method C

9.4.1 General comments

Method C is, in general, sufficiently accurate for industrial gears. To determine the transverse load factors $K_{H\alpha\text{-}C}$, $K_{F\alpha\text{-}C}$ the gear accuracy grade, specific loading, gear type and running-in behaviour are required. The running-in behaviour is expressed by material and type of heat treatment (see Figure 6 or Figure 7).

9.4.2 Premises, assumptions

The following assumptions are valid for method C:

— a transverse contact ratio of $1{,}2 < \varepsilon_{v\alpha} < 1{,}9$ applies to tooth stiffness (see ISO 6336-1[2]);

— stiffness values of $c_\gamma = 20$ N/(mm·µm) according to Formula (11) or $c' = 14$ N/(mm·µm) according to Formula (17);

— a single pitch deviation is assigned to each gear accuracy grade. With this assumption, transverse load distribution factors are obtained which are on the safe side for most applications, i.e. in case of mean and high specific loadings, as well as in case of specific loadings $F_{vmt}\, K_A / b_{v,eff} < 100$ N/mm.

9.4.3 Determination of the factors

$K_{H\alpha\text{-}C}$ and $K_{F\alpha\text{-}C}$ shall be taken from Table 5.

Attention — If the gear accuracy grades are different for pinion and wheel, the worse one shall be used.

Table 5 — Transverse load distribution factors, $K_{H\alpha\text{-c}}$ and $K_{F\alpha\text{-c}}$

<table>
<tr><th colspan="3">Specific loading
$F_{vmt}\,K_A/b_{v,eff}$</th><th colspan="7">≥100 N/mm</th><th><100 N/mm</th></tr>
<tr><th colspan="3">Gear accuracy grade
(see 5.3.2)</th><th>5 and better</th><th>6</th><th>7</th><th>8</th><th>9</th><th>10</th><th>11</th><th>all accuracy grades</th></tr>
<tr><td rowspan="4">Surface hardened</td><td rowspan="2">Straight bevel gears</td><td>$K_{H\alpha}$</td><td rowspan="2" colspan="2">1,0</td><td rowspan="2">1,1</td><td rowspan="2">1,2</td><td colspan="4">(B1):$1/Z_{LS}^2$ or 1,2
(B2):$1/\varepsilon_{NI}$ or 1,2
whichever is the greater</td></tr>
<tr><td>$K_{F\alpha}$</td><td colspan="4">(B1):$1/Y_{LS}$ or 1,2
(B2):$1/\varepsilon_{N}$ or 1,2
whichever is the greater</td></tr>
<tr><td rowspan="2">Helical and spiral bevel gears</td><td>$K_{H\alpha}$</td><td rowspan="2">1,0</td><td rowspan="2">1,1</td><td rowspan="2">1,2</td><td rowspan="2">1,4</td><td rowspan="2" colspan="4">$\varepsilon_{v\alpha n}$ or 1,4 whichever is the greater</td></tr>
<tr><td>$K_{F\alpha}$</td></tr>
<tr><td rowspan="4">Not surface hardened</td><td rowspan="2">Straight bevel gears</td><td>$K_{H\alpha}$</td><td rowspan="2" colspan="3">1,0</td><td rowspan="2">1,1</td><td rowspan="2">1,2</td><td colspan="3">(B1):$1/Z_{LS}^2$ or 1,2
(B2):$1/\varepsilon_{NI}$ or 1,2
whichever is the greater</td></tr>
<tr><td>$K_{F\alpha}$</td><td colspan="3">(B1):$1/Y_{LS}$ or 1,2
(B2):$1/\varepsilon_{N}$ or 1,2
whichever is the greater</td></tr>
<tr><td rowspan="2">Helical and spiral bevel gears</td><td>$K_{H\alpha}$</td><td rowspan="2" colspan="2">1,0</td><td rowspan="2">1,1</td><td rowspan="2">1,2</td><td rowspan="2">1,4</td><td rowspan="2" colspan="3">$\varepsilon_{v\alpha n}$ or 1,4
whichever is the greater</td></tr>
<tr><td>$K_{F\alpha}$</td></tr>
<tr><td colspan="11">NOTE For Z_{LS}, ε_{NI} and Y_{LS}, ε_N see 9.3.3. (B1) and (B2) stands for method B1 and method B2.</td></tr>
</table>

9.5 Running-in allowance, y_α

The running-in allowance, y_α, is the amount due to running-in by which the mesh alignment error is reduced from the start of the operation. In the absence of direct experience, y_α may be taken from Figure 6 or Figure 7.

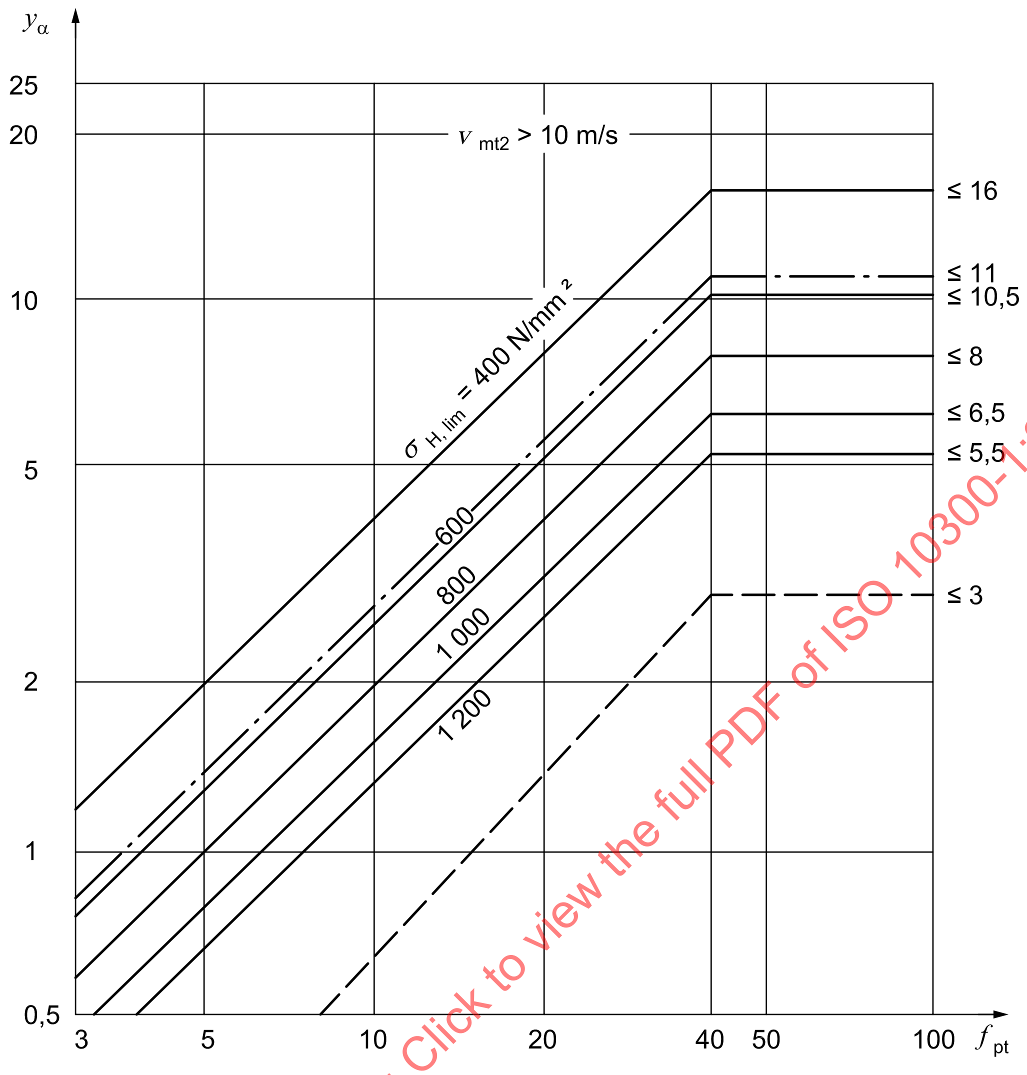

Key

f_{pt} single pitch deviation (µm)

y_α running-in allowance (µm)

——————— structural and through hardened steel

——·——·—— grey cast iron

— — — — — case hardened and nitrided steel

Figure 6 — Running-in allowance, y_α, of gear pairs with a tangential speed of v_{mt2} > 10 m/s

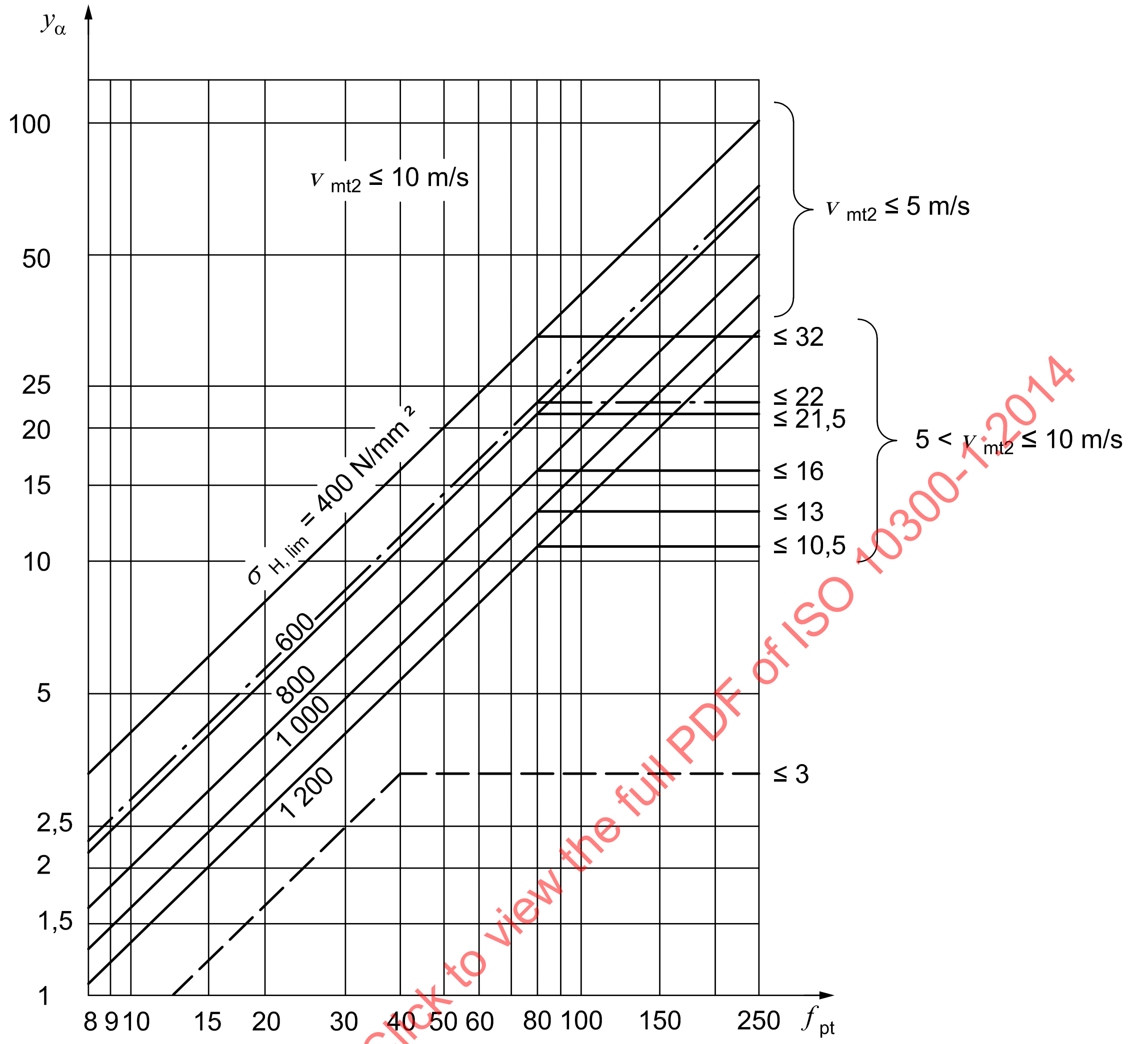

Key

f_{pt}	single pitch deviation (µm)
y_{α}	running-in allowance (µm)
————	structural and through hardened steel
— · — · —	grey cast iron
— — — —	case hardened and nitrided steel

Figure 7 — Running-in allowance, y_{α}, of gear pairs with a tangential speed of $v_{mt2} \leq 10$ m/s

The following equations, representing the curves in Figures 6 and 7, may be used for the calculation (where f_{pt} is single pitch deviation, see 9.3.1).

For through hardened steels:

$$y_{\alpha} = \frac{160}{\sigma_{H,lim}} f_{pt} \tag{41}$$

for $v_{mt2} \leq 5$ m/s:	without restriction;
for 5 m/s < $v_{mt2} \leq 10$ m/s:	$y_{\alpha} \leq 12\,800/\sigma_{H,lim}$;
for $v_{mt2} > 10$ m/s:	$y_{\alpha} \leq 6\,400/\sigma_{H,lim}$.

For grey cast iron:

$$y_\alpha = 0{,}275\, f_{pt} \tag{42}$$

for $v_{mt2} \leq 5$ m/s: without restriction;

for 5 m/s < $v_{mt2} \leq 10$ m/s: $y_\alpha \leq 22$ µm;

for $v_{mt2} > 10$ m/s: $y_\alpha \leq 11$ µm.

For case hardened and nitrided gears:

$$y_\alpha = 0{,}075\, f_{pt} \tag{43}$$

for all speeds with the restriction: $y_\alpha \leq 3$ µm.

If materials of pinion and wheel are different, a mean value for y_α shall be calculated:

$$y_\alpha = \frac{y_{\alpha 1} + y_{\alpha 2}}{2} \tag{44}$$

wherein $y_{\alpha 1}$ is to be determined for the pinion material and $y_{\alpha 2}$ for the wheel material.

Annex A
(normative)

Calculation of virtual cylindrical gears — Method B1

A.1 General

Approved rating procedures for pitting resistance and bending strength of bevel and hypoid gears which can serve as a standard are based on virtual cylindrical gears. The main reason is that the necessary allowable stress values can be taken from tests of cylindrical gears which are easier to get and statistically more reliable than those from the fewer tests of bevel or hypoid gears.

The decisive requirement for this approach is a good equivalence between the meshing conditions of bevel or hypoid gears and of their corresponding virtual cylindrical gears. In order to ensure this, exact tooth contact analysis calculations (TCA) were carried out for a broad variety of bevel and hypoid gears and compared with the meshing conditions of the corresponding virtual cylindrical gears. By this means the known formulae for bevel gears without offset were confirmed and new extended formulae including hypoid gears were defined. The latter refers to major parameters of virtual cylindrical gears, such as helix angle, face width, contact ratio, radius of relative curvature.

Besides, the virtual cylindrical gears for hypoids were developed such that with decreasing offset values, they continuously approximate to the known dimensions of those for spiral bevel gears without offset. The advantage is that also the calculated load capacities of these hypoid gears approximate to the proven good results of spiral bevel gears.

So, Annex A contains geometric relations for generating the data of the required virtual cylindrical gears. The gear data presented here apply exclusively to gears with ($x_{hm1} + x_{hm2}$) = 0. The initial bevel or hypoid gear data necessary for these calculations should conform to ISO 23509.

A.2 Data of virtual cylindrical gears in transverse section (suffix v)

A.2.1 General

If a transverse section of a bevel gear tooth at midface is developed into the sectional plane, a virtual cylindrical gear is obtained with nearly involute teeth. This is standard practice for bevel gears without hypoid offset (see Figure A.2). For hypoid gears which are geometrically the most general type of gearing, a similar procedure is applicable. Looking at Figure A.1, a schematic diagram of hypoid gears (see also Figure A.2 of ISO 23509:2006) shows a common tangential plane T between both pitch cones with diameters d_{m1} and d_{m2}, which contact each other at the mean point P. Besides, both pitch cones contact with the tangential plane T along lines which are designated as mean cone distances R_{m1} and R_{m2} and include the offset angle ζ_{mp}.

A normal line to the plane T, erected in the mean point, intersects with the pinion axis at n_P and with the wheel axis at n_G. This line corresponds to line Q of Figure A.2 representing the centre distance a_v of virtual cylindrical gears. With hypoid gears, however, the pinion axis and wheel axis are not in the same plane. In order to get virtual cylindrical gears with parallel axes, an approximation is made by giving both axes the direction, which divides the offset angle ζ_{mp} into half.

It is not assumed that thus-defined virtual cylindrical gears have the same meshing conditions as hypoid gears. This is adjusted afterwards by several appropriate correction factors such as the hypoid factor Z_{Hyp} which accounts for the influence of the lengthwise sliding of hypoid gear teeth. However, virtual cylindrical gears supply the required geometrical basis to achieve a practicable rating system for all types of bevel gears.

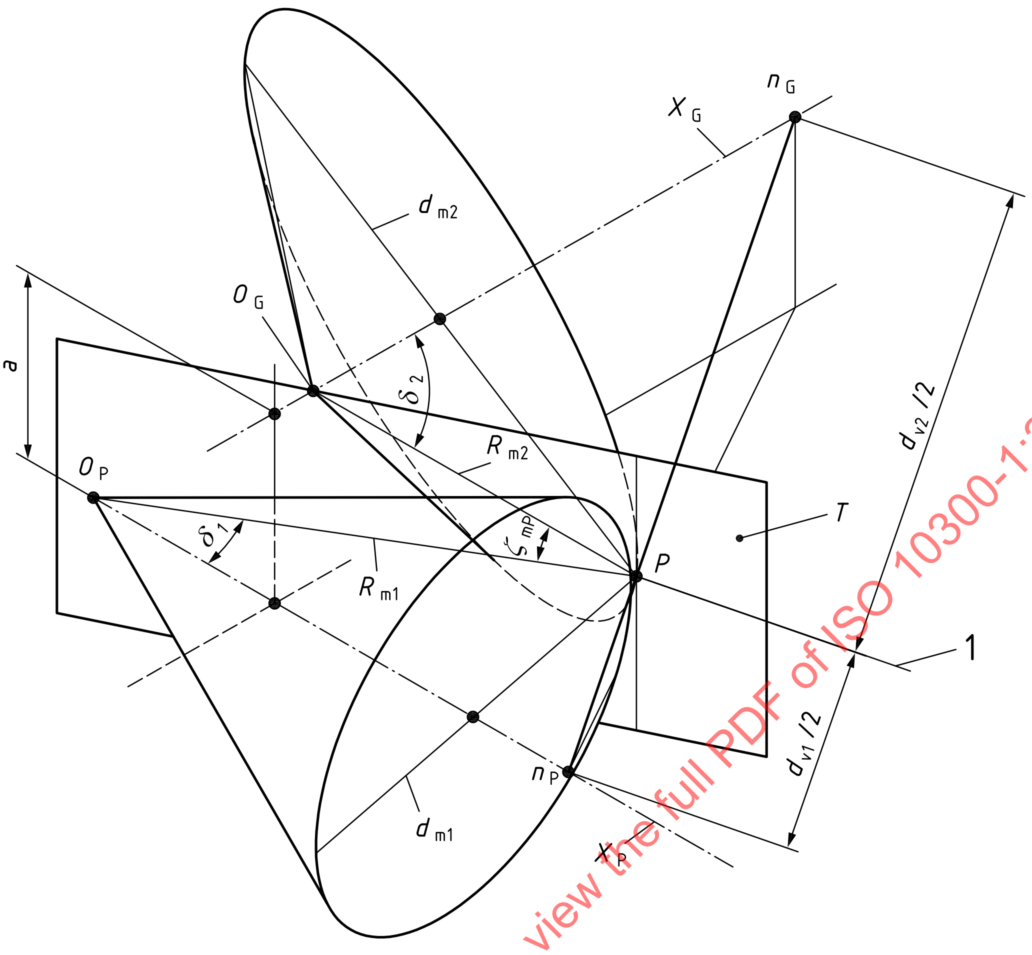

Key

1 bisecting line of the offset angle ζ_{mp}

Figure A.1 — Schematic diagram of hypoid gear

A.2.2 Determination of the diameters, d_v:

Reference diameter, d_v:

$$d_{v1,2} = \frac{d_{m1,2}}{\cos\delta_{1,2}} \tag{A.1}$$

for hypoid gears:

$$d_{m2} \neq u\, d_{m1} \tag{A.2}$$

for a = 0 and Σ = 90°:

$$d_{v1} = d_{m1} \frac{\sqrt{u^2 + 1}}{u} \tag{A.3}$$

$$d_{v2} = u^2\, d_{v1} \tag{A.4}$$

Centre distance, a_v:

$$a_v = \left(d_{v1} + d_{v2}\right) / 2 \tag{A.5}$$

Tip diameter, d_{va}:

$$d_{va1,2} = d_{v1,2} + 2\, h_{am1,2} \tag{A.6}$$

Root diameter, d_{vf}:

$$d_{vf1,2} = d_{v1,2} - 2\, h_{fm1,2} \tag{A.7}$$

From Figure A.1 it is also conceivable that the hypoid offset, a, and simultaneously the offset angle ζ_{mp} decrease until at a = 0 the special case of bevel gears without offset is reached and the cone distances R_{m1} and R_{m2} coincide. Then, the well-known former parameters of virtual cylindrical gears are valid again as given in Figure A.2.

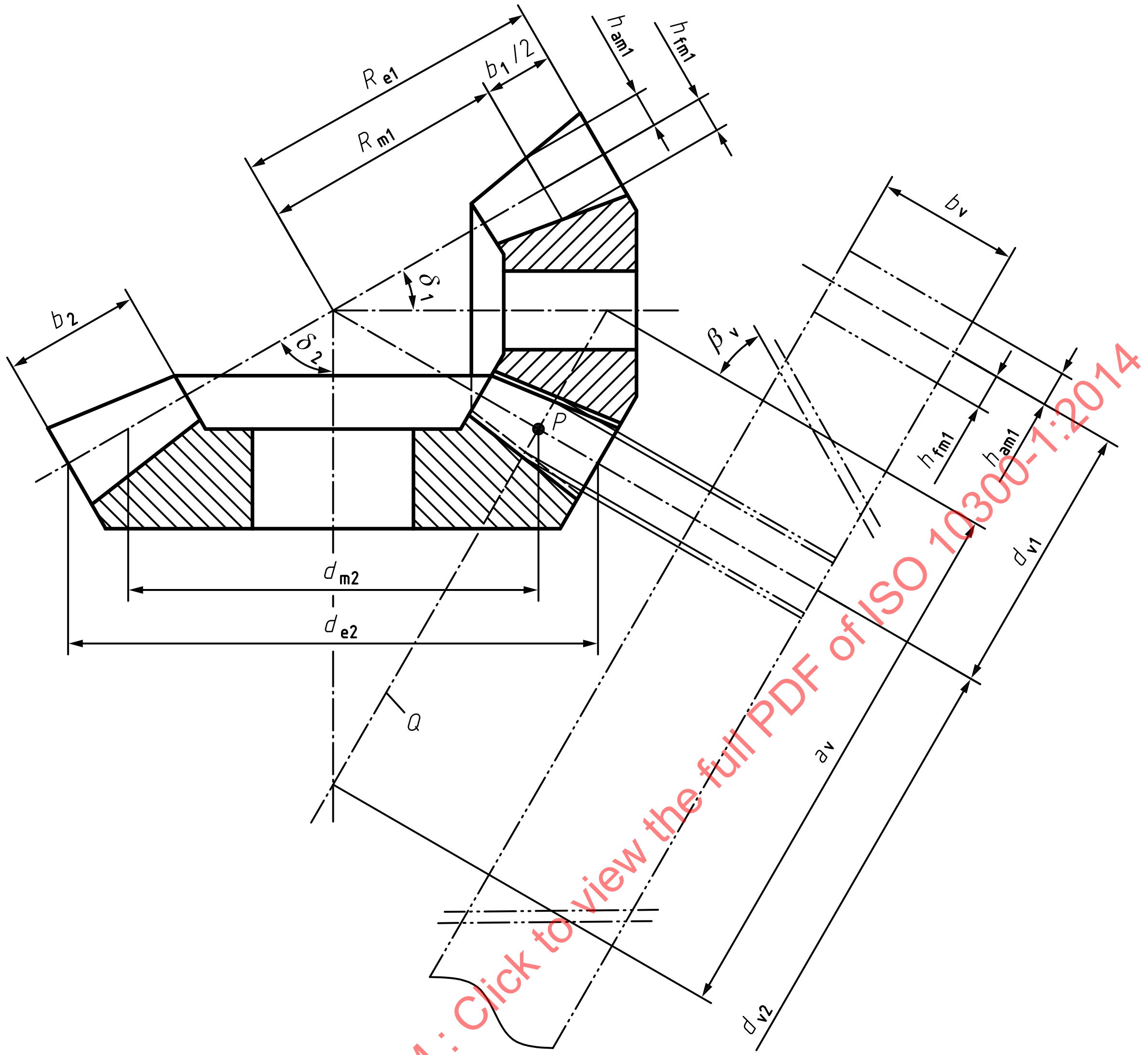

Figure A.2 — Bevel gears without offset and their corresponding virtual cylindrical gears

A.2.3 Determination of the helix angle, β_v

For bevel gears without offset, the helix angle β_v of virtual cylindrical gears is equal to the spiral angle of the pinion β_{m1} and the wheel β_{m2} because $\beta_{m1} = \beta_{m2}$. However, this is not true with hypoid gears where $\beta_{m1} = \beta_{m2} + \zeta_{mp}$ (see ISO 23509). In order to find the one helix angle for the virtual cylindrical gear pair, it is referred to Figure A.1 where the bisecting line of the angle ζ_{mp} defines the direction of the virtual pinion axis and wheel axis. Then, the pinion helix angle is $\beta_{m1} - \zeta_{mp}/2$, is equal to the wheel helix angle $\beta_{m2} + \zeta_{mp}/2$, and both are equal to the helix angle β_v of the virtual cylindrical gear pair.

On this basis a comparison of the meshing conditions mentioned in A.1 was applied. The inclination angle β_B between the contact line and the pitch line in the mean point was used as a representative parameter in this case. It turned out that the inclination angle β_B calculated by TCA for any bevel or hypoid gear has nearly the same value as calculated for the corresponding virtual cylindrical gear with helix angle β_v which is the arithmetic mean value of both spiral angles β_{m1} and β_{m2}.

NOTE In this context, contact line means the major axis of the Hertzian contact ellipse under load.

Helix angle, β_v:

$$\beta_v = \frac{\beta_{m1} + \beta_{m2}}{2} \tag{A.8}$$

Base diameter, d_{vb}:

$$d_{vb1,2} = d_{v1,2} \cos\alpha_{vet} \tag{A.9}$$

where:

$$\alpha_{vet} = \arctan\left(\tan\alpha_e / \cos\beta_v\right) \tag{A.10}$$

a) $\alpha_e = \alpha_{eD}$ for drive side (see ISO 23509);

b) $\alpha_e = \alpha_{eC}$ for coast side (see ISO 23509).

Transverse module, m_{vt}:

$$m_{vt} = m_{mn} / \cos\beta_v \tag{A.11}$$

Number of teeth, z_v:

$$z_{v1,2} = d_{v1,2} / m_{vt} \tag{A.12}$$

Gear ratio, u_v:

$$u_v = z_{v2} / z_{v1} \tag{A.13}$$

for $a = 0$ and $\Sigma = 90°$: $z_{v1} = z_1 \frac{\sqrt{u^2 + 1}}{u}$ (A.14)

$$z_{v2} = z_2 \sqrt{u^2 + 1} \tag{A.15}$$

Helix angle at base circle, β_{vb}:

$$\beta_{vb} = \arcsin\left(\sin\beta_v \cos\alpha_e\right) \tag{A.16}$$

Transverse base pitch, p_{vet}:

$$p_{vet} = \pi\ m_{mn} \cos\alpha_{vet} / \cos\beta_v \tag{A.17}$$

Length of path of contact, $g_{v\alpha}$:

$$g_{v\alpha} = \frac{1}{2}\left[\left(\sqrt{d_{va1}{}^2 - d_{vb1}{}^2} - d_{v1} \sin\alpha_{vet}\right) + \left(\sqrt{d_{va2}{}^2 - d_{vb2}{}^2} - d_{v2} \sin\alpha_{vet}\right)\right] \tag{A.18}$$

A.2.4 Determination of the face width, b_v

Whereas the face width of virtual cylindrical gears and of their corresponding bevel gears without offset have the same size ($b_v = b$, see Figure A.2), this is not true for hypoid gears. Before the face width b_v is calculated, the effective face width $b_{v,eff}$ of the virtual cylindrical gear pair shall be determined.

For that purpose, the length of the contact pattern $b_{2,\text{eff}}$, which is measured in the direction of the wheel face width, is used.

Simplified, it is assumed that the theoretical zone of action of the hypoid wheel is not arched but developed into a parallelogram and then projected on to the common pitch plane T as shown in Figure A.3 by dotted bold lines. The side lines of this zone of action around mean point P are vertical to the wheel axis which in this view coincides with the cone distance R_{m2}. The other two boundary lines are parallel to the instantaneous axis of helical relative motion of the hypoid gear pair which is given by the angle ϑ_{mp}.

The zone of action of the corresponding virtual cylindrical gear pair is the greatest possible parallelogram (bold lines in Figure A.3) inscribed in the theoretical zone of action of the wheel whereby the side lines now are vertical to the axis of roll of the virtual cylindrical gear pair given by the angle $\zeta_{\text{mp}}/2$. The width of this smaller parallelogram appears in the given view in true length and it is the effective face width $b_{\text{v eff}}$ of the virtual cylindrical gear pair. To get the complete zone of action in true size, the given top view is projected into the plane inclined by the effective pressure angle, α_{vet}, of the active flank in which the path of contact is also in true size (see key item 4 of Figure A.3).

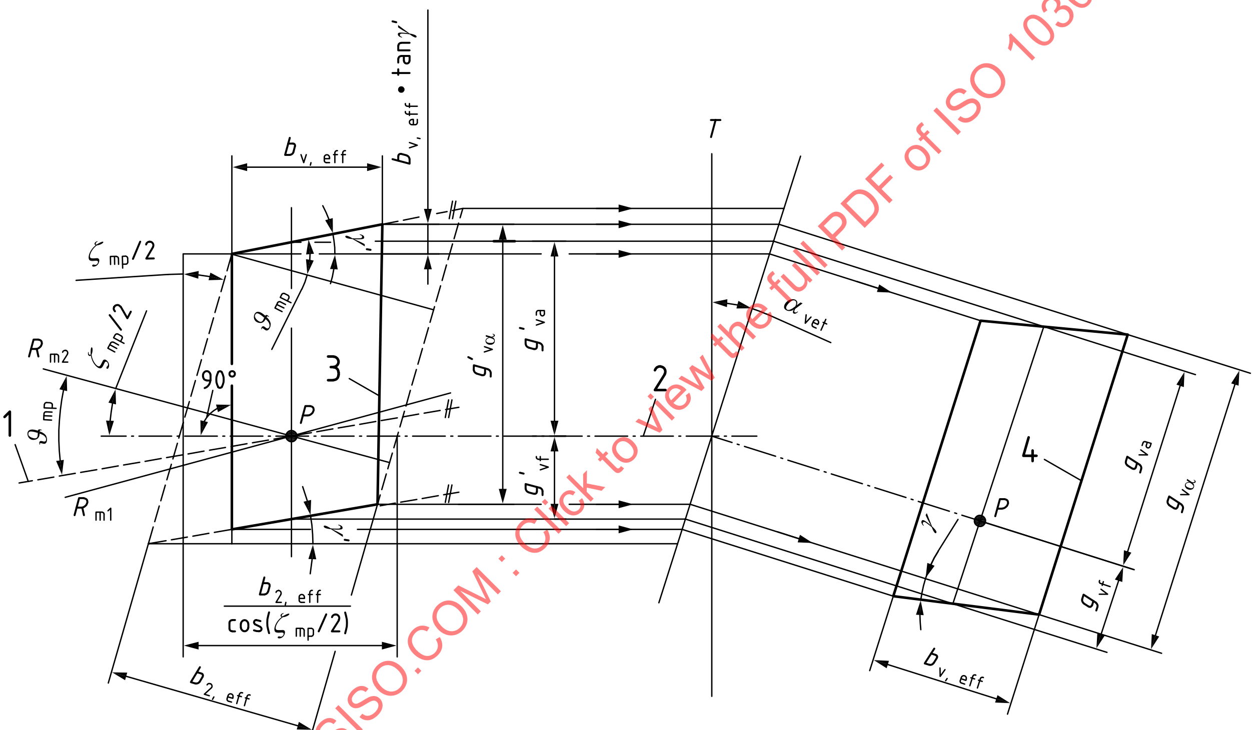

Key

1 axis of relative helical motion of the hypoid gears

2 axis of roll of the virtual cylindrical gears

3 projected zone of action in tangential plane (dimensions of bevel gears)

4 zone of action in meshing plane (dimensions of virtual cylindrical gears)

Figure A.3 — Simplified zone of action for virtual cylindrical gears

The following Formula (A.19) is derived from Figure A.3:

Effective face width, $b_{\text{v,eff}}$:

$$b_{\text{v,eff}} = \frac{\left(b_{2,\text{eff}} / \cos\left(\zeta_{\text{mp}}/2\right) - g_{\text{v}\alpha} \cos\alpha_{\text{vet}} \tan\left(\zeta_{\text{mp}}/2\right)\right)}{1 - \tan\gamma' \tan\left(\zeta_{\text{mp}}/2\right)} \tag{A.19}$$

where:

$$\gamma' = \vartheta_{mp} - \zeta_{mp}/2 \tag{A.20}$$

$$\vartheta_{mp} = \arctan\left(\sin\delta_2 \tan\zeta_m\right) \tag{A.21}$$

α_{vet} is the effective pressure angle of the virtual cylindrical gears calculated for the active flank, see Formula (A.10);

for ζ_{mp} and ζ_m see ISO 23509.

$b_{2,eff}$ is the effective width of the contact pattern under a certain load. It should be derived from measurements or TCA, at the preliminary design stage $b_{2,eff} = 0{,}85\ b_2$ is a reasonable estimate.

In a second step, the face width b_v is defined:

$$b_v = b_2 \frac{b_{v,eff}}{b_{2,eff}} \tag{A.22}$$

A.2.5 Comparison of meshing conditions

The parallelogram as zone of action determined for the virtual cylindrical gear pair is now compared with the real contact lines and pattern calculated by a TCA of the bevel gear set. Both zones of action are projected into a plane vertical to the wheel axis and then superposed for illustration. Six such sample plots, derived from three gear sets with different offset values a, are arranged in Table A.1, considering both flanks (drive side and coast side). As a reference, each little plot gives the axis of roll of virtual cylindrical gears and the lines of mean cone distances of pinion and wheel which intersect in the respective mean point P.

In addition, the parallelogram of the virtual zone of action contains three representative straight contact lines (bold lines). They fit angularly very well with the calculated curved contact lines which are drawn thicker where they form the contact pattern. Also, each of these calculated contact patterns is well covered in size and position by the parallelogram of the respective virtual cylindrical gear, which means that the equivalence of the meshing conditions between bevel gears and their virtual cylindrical gears is very good for a rating system.

It was found that the former ellipse, inscribed in the zone of action, produces no better results than the newly defined parallelogram. It seems that the major axis of the ellipse does not always have to be parallel to the axis of the virtual cylindrical gear, but should at least be turned by an angle, which would be very difficult to calculate.

Table A.1 — Exemplary zones of action of virtual cylindrical gear pairs and calculated contact patterns of the bevel gear sets in a projection parallel to the wheel axis

Actual flank	Hypoid offset		
	a = 0 mm	a = 15 mm	a = 30 mm
Drive side	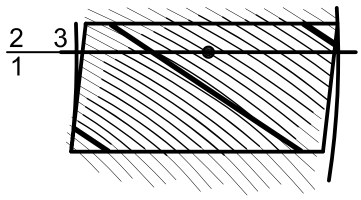	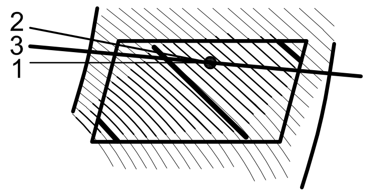	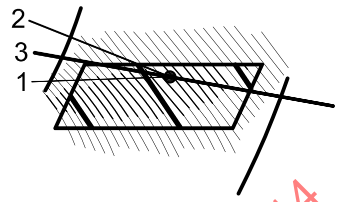
Coast side	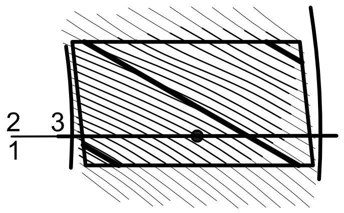	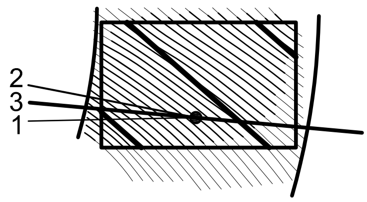	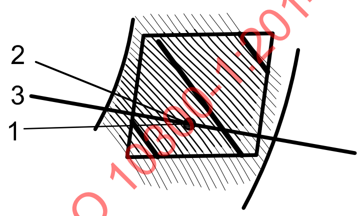

Key

1 mean cone distance pinion

2 mean cone distance wheel

3 axis of roll

A.2.6 Determination of contact ratios, ε_{v}

Transverse contact ratio, $\varepsilon_{\mathrm{v\alpha}}$:

$$\varepsilon_{\mathrm{v\alpha}} = g_{\mathrm{v\alpha}} / p_{\mathrm{vet}} \tag{A.23}$$

Face contact ratio, $\varepsilon_{\mathrm{v\beta}}$:

$$\varepsilon_{\mathrm{v\beta}} = \frac{b_{\mathrm{v,eff}} \sin \beta_{\mathrm{v}}}{\pi \, m_{\mathrm{mn}}} \tag{A.24}$$

The transverse and face contact ratios calculated with Formulae (A.23) and (A.24) for the virtual cylindrical gear are determinant for the load capacity calculation. But it is possible that they deviate from the ratios calculated on the basis of the real dimensions of the bevel gears or on the basis of a TCA.

Virtual contact ratio, $\varepsilon_{\mathrm{v\gamma}}$:

$$\varepsilon_{\mathrm{v\gamma}} = \varepsilon_{\mathrm{v\alpha}} + \varepsilon_{\mathrm{v\beta}} \tag{A.25}$$

A.2.7 Determination of the length of contact lines, l_{b}

When the tooth contact has been suitably developed, the full load contact should not extend beyond the boundary of the assumed parallelogram (see Figure A.4). Normally the contact lines are shorter than they theoretically could be because of the crowning of the flanks in profile and lengthwise directions. This is considered with the correction factor C_{lb} which reduces the length of the contact lines by an elliptical function (see Figure A.5).

Formulae (A.26) to (A.36) shall be calculated, according to Table A.2, for:

a) the tip contact line with $f = f_{\mathrm{t}}$;

b) the middle contact line, l_{bm}, with $f = f_{\mathrm{m}}$;

c) the root contact line with $f = f_r$.

Table A.2 — Distance *f* of the tip, middle and root contact line in the zone of action

–		Surface durability	Tooth root strength
$\varepsilon_{v\beta} = 0$	f_t	$-(p_{vet} - 0{,}5\, p_{vet}\, \varepsilon_{v\alpha}) \cos\beta_{vb} + p_{vet} \cos\beta_{vb}$	$(p_{vet} - 0{,}5\, p_{vet}\, \varepsilon_{v\alpha}) \cos\beta_{vb} + p_{vet} \cos\beta_{vb}$
	f_m	$-(p_{vet} - 0{,}5\, p_{vet}\, \varepsilon_{v\alpha}) \cos\beta_{vb}$	$(p_{vet} - 0{,}5\, p_{vet}\, \varepsilon_{v\alpha}) \cos\beta_{vb}$
	f_r	$-(p_{vet} - 0{,}5\, p_{vet}\, \varepsilon_{v\alpha}) \cos\beta_{vb} - p_{vet} \cos\beta_{vb}$	$(p_{vet} - 0{,}5\, p_{vet}\, \varepsilon_{v\alpha}) \cos\beta_{vb} - p_{vet} \cos\beta_{vb}$
$0 < \varepsilon_{v\beta} < 1$	f_t	$-(p_{vet} - 0{,}5\, p_{vet}\, \varepsilon_{v\alpha}) \cos\beta_{vb} (1-\varepsilon_{v\beta}) + p_{vet} \cos\beta_{vb}$	$(p_{vet} - 0{,}5\, p_{vet}\, \varepsilon_{v\alpha}) \cos\beta_{vb} (1-\varepsilon_{v\beta}) + p_{vet} \cos\beta_{vb}$
	f_m	$-(p_{vet} - 0{,}5\, p_{vet}\, \varepsilon_{v\alpha}) \cos\beta_{vb} (1 - \varepsilon_{v\beta})$	$(p_{vet} - 0{,}5\, p_{vet}\, \varepsilon_{v\alpha}) \cos\beta_{vb} (1 - \varepsilon_{v\beta})$
	f_r	$-(p_{vet} - 0{,}5\, p_{vet}\, \varepsilon_{v\alpha}) \cos\beta_{vb} (1 - \varepsilon_{v\beta}) - p_{vet} \cos\beta_{vb}$	$(p_{vet} - 0{,}5\, p_{vet}\, \varepsilon_{v\alpha}) \cos\beta_{vb} (1 - \varepsilon_{v\beta}) - p_{vet} \cos\beta_{vb}$
$\varepsilon_{v\beta} \geq 1$	f_t	$+ p_{vet} \cos\beta_{vb}$	$+ p_{vet} \cos\beta_{vb}$
	f_m	0	0
	f_r	$- p_{vet} \cos\beta_{vb}$	$- p_{vet} \cos\beta_{vb}$

NOTE Because of the symmetry of the contact area with respect to the point M, a contact line with the distance *f* has the same length compared to a contact line with the distance $-f$. Hence the sum of the length of the three considered contact lines is independent of the sign of distance *f*.

In this case, $f_{m\,(pitting)} = -f_{m\,(tooth\ root)}$; $f_{r\,(pitting)} = -f_{t\,(tooth\ root)}$ and $f_{t\,(pitting)} = -f_{r\,(tooth\ root)}$. Together with the symmetry of load distribution according to ISO 10300-2:2014, Figure 2, this leads in total to load sharing factors for pitting, Z_{LS}, and for tooth root, Y_{LS}, where $Y_{LS} = Z_{LS}^2$.

Length of contact line, l_b:

$$l_b = l_{b0} \left(1 - C_{lb}\right) \tag{A.26}$$

for C_{lb} = correction factor, see Formula (A.34).

Theoretical length of contact line, l_{b0}:

$$l_{b0} = \sqrt{\left(x_1 - x_2\right)^2 + \left(y_1 - y_2\right)^2} \tag{A.27}$$

where

$$x_1 = \frac{f \cos\beta_{vb} + \tan\beta_{vb} \left(f \sin\beta_{vb} + \dfrac{b_{v,eff}}{2} \right) + \dfrac{1}{2} \left(g_{v\alpha} + b_{v,eff} \tan\gamma \right)}{\tan\gamma + \tan\beta_{vb}} \tag{A.28}$$

$$x_2 = \frac{f \cos\beta_{vb} + \tan\beta_{vb} \left(f \sin\beta_{vb} + \dfrac{b_{v,eff}}{2} \right) - \dfrac{1}{2} \left(g_{v\alpha} + b_{v,eff} \tan\gamma \right)}{\tan\gamma + \tan\beta_{vb}} \tag{A.29}$$

$$y_{1,2} = -x_{1,2} \tan\beta_{vb} + f \cos\beta_{vb} + \tan\beta_{vb} \left(f \sin\beta_{vb} + \frac{b_{v,eff}}{2} \right) \tag{A.30}$$

Attention — If $x_{1,2} < 0$: $x_{1,2} = 0$ and if $x_{1,2} > b_{v,eff}$: $x_{1,2} = b_{v,eff}$.

The maximum distances from the middle contact line are calculated according to Figure A.4:

$$f_{maxB} = \frac{1}{2} \left[g_{v\alpha} + b_{v,eff} \left(\tan\gamma + \tan\beta_{vb} \right) \right] \cos\beta_{vb} \tag{A.31}$$

$$f_{max0} = \frac{1}{2}\left[g_{v\alpha} - b_{v\,eff}\left(\tan\gamma + \tan\beta_{vb}\right)\right]\cos\beta_{vb} \tag{A.32}$$

with

$$\tan\gamma = \tan\gamma' / \cos\alpha_{vet} \tag{A.33}$$

Attention — If $f_{maxB} > f_{max0}$: $f_{max} = f_{maxB}$ else $f_{max} = f_{max0}$.

Correction factor, C_{lb}:

$$C_{lb} = \sqrt{\left(1 - \left(\frac{f}{f_{max}}\right)^2\right)\left(1 - \sqrt{\frac{b_{v,eff}}{b_v}}\right)^2} \tag{A.34}$$

Figure A.4 shows the general definitions of values for calculating the theoretical length of lines of contact l_{b0}.

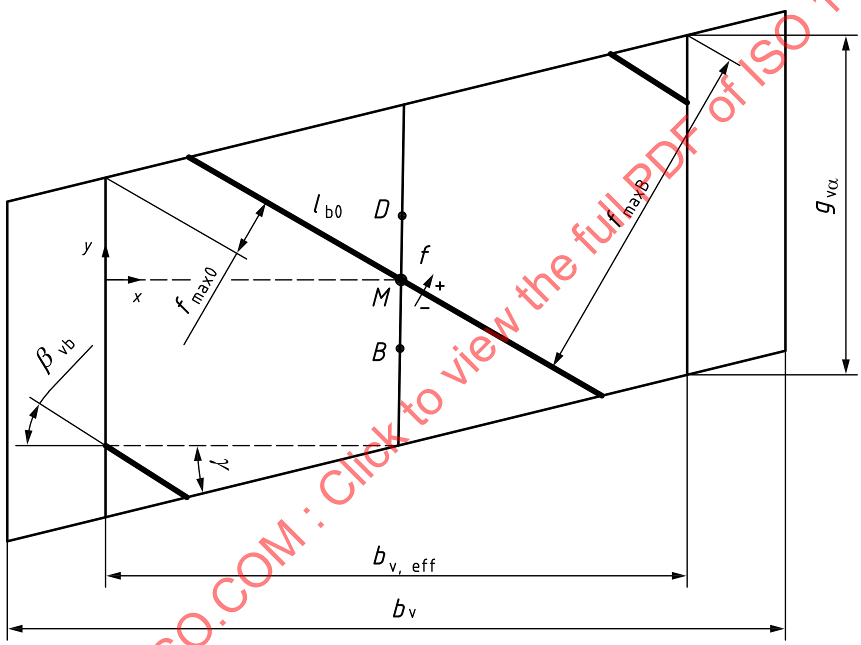

Key

D outer point of single contact

M centre of the zone of action

B inner point of single contact

Figure A.4 — General definition of length of contact lines

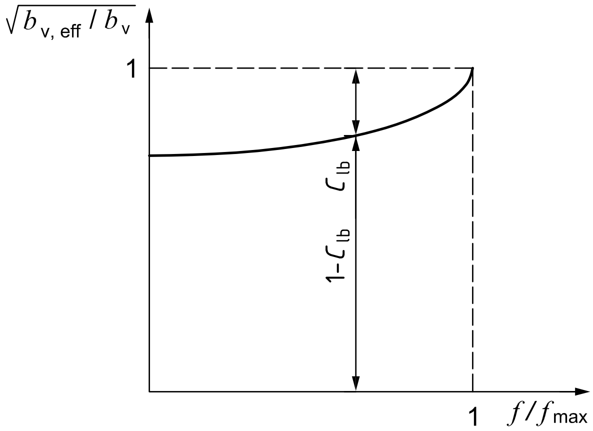

Figure A.5 — Correction factor, C_{lb}

A.2.8 Determination of the radius of relative curvature, ρ_{rel} for the contact stress calculation:

Radius of relative curvature vertical to the contact line, ρ_{rel}:

$$\rho_{rel} = \left|\rho_t\right| \cos^2 \beta_B \tag{A.35}$$

Inclination angle of contact line, β_B:

$$\beta_B = \arctan\left(\tan \beta_v \sin \alpha_e\right) \tag{A.36}$$

where

$\alpha_e = \alpha_{eD}$ for drive side (see ISO 23509);

$\alpha_e = \alpha_{eC}$ for coast side (see ISO 23509).

Radius of relative curvature in normal section at the mean point, ρ_t; see Reference [6]:

a) Drive side:

$\rho_t =$

$$\left[\frac{1}{\cos\alpha_{nD}\left(\tan\alpha_{nD} - \tan\alpha_{lim}\right) + \tan\zeta_{mp}\tan\beta_B}\frac{\cos\beta_{m1}\cos\beta_{m2}}{\cos\zeta_{mp}} \cdot \left(\frac{1}{R_{m2}\tan\delta_2} + \frac{1}{R_{m1}\tan\delta_1}\right)\right]^{-1} \tag{A.37a}$$

b) Coast side:

$\rho_t =$

$$\left[\frac{1}{\cos\alpha_{nC}\left(\tan(-\alpha_{nC}) - \tan\alpha_{lim}\right) - \tan\zeta_{mp}\tan\beta_B}\frac{\cos\beta_{m1}\cos\beta_{m2}}{\cos\zeta_{mp}} \cdot \left(\frac{1}{R_{m2}\tan\delta_2} + \frac{1}{R_{m1}\tan\delta_1}\right)\right]^{-1} \tag{A.37b}$$

A.3 Data of virtual cylindrical gear in normal section (suffix vn)

Number of teeth z_{vn} of virtual spur gears:

$$z_{vn1} = \frac{z_{v1}}{\cos^2\beta_{vb}\cos\beta_v} \tag{A.38}$$

$$z_{vn2} = u_v z_{vn1} \tag{A.39}$$

Reference diameter d_{vn}:

$$d_{vn1,2} = \frac{d_{v1,2}}{\cos^2 \beta_{vb}} = z_{vn1,2} m_{mn} \tag{A.40}$$

Tip diameter d_{van}:

$$d_{van1,2} = d_{vn1,2} + d_{va1,2} - d_{v1,2} = d_{vn1,2} + 2h_{am1,2} \tag{A.41}$$

Base diameter d_{vbn}:

$$d_{vbn1,2} = d_{vn1,2} \cos\alpha_e = z_{vn1,2\ D,C} m_{mn} \cos\alpha_e \tag{A.42}$$

Profile contact ratio $\varepsilon_{v\alpha n}$:

$$\varepsilon_{v\alpha n} = \varepsilon_{v\alpha} / \cos^2 \beta_{vb} \tag{A.43}$$

Attention — Hypoid gears with different effective pressure angles for drive and coast side have different virtual cylindrical gears in normal section. Therefore, z_{vn}, d_{van} and d_{vbn} should be calculated separately for drive flank (suffix D) and coast flank (suffix C).